We are IntechOpen,
the world's leading publisher of
Open Access books
Built by scientists, for scientists

4,800
Open access books available

122,000
International authors and editors

135M
Downloads

154
Countries delivered to

Our authors are among the

TOP 1%
most cited scientists

12.2%
Contributors from top 500 universities

Interested in publishing with us?
Contact book.department@intechopen.com

Numbers displayed above are based on latest data collected.
For more information visit www.intechopen.com

Conducting Polymer-Metal Nanocomposite Coating on Fibers

Syuji Fujii[1], Mizuho Kodama[1], Soichiro Matsuzawa[2],
Hiroyuki Hamasaki[1], Atsushi Ohtaka[1] and Yoshinobu Nakamura[1,3]
[1]Department of Applied Chemistry, Faculty of Engineering
Osaka Institute of Technology, Osaka
[2]Graduate School of Engineering Osaka Institute of Technology, Osaka
[3]Nanomaterials Microdevices Research Center,Osaka Institute of Technology, Osaka
Japan

1. Introduction

Conducting polymers continue to be the focus of active research in diverse fields including electronics (Burroughes et al., 1988; Sailor et al., 1990; Gustafsson et al., 1992; Zhang et al., 1994), energy storage (Conway, 1991; Geniès, 1991; Li et al., 1991), catalysis (Andrieux et al., 1982 ; Bull et al., 1983; Hable et al., 1993), chemical sensing (Josowicz et al., 1986; Heller, 1992; Gardner et al., 1993; Kuwabata et al., 1994; Freund et al., 1995) and biochemistry (Miller, 1988; Guimard et al., 2007). Despite the promise of these new materials and their widespread study, the scope of commercial uses remains small and relatively few viable technologies have emerged from the laboratory proof-of-concept stage. Limitations of processability such as low mechanical strength, poor flexibility and high cost have prevented conducting polymers from making significant commercial impact. In order to improve the processability of the conducting polymers, several approaches have been developed over the years: (1) synthesis of soluble conducting polymers by the addition of bulky side chains along the backbone (Wang et al., 2003), (2) synthesis in the form of colloidal dispersions by dispersion and emulsion polymerizations (Armes, 1998; Chehimi et al., 2004), (3) the use of metastable mixtures of monomer and oxidant that enable processability followed by *in situ* polymerization initiated by solvent evaporation (Grimaldo et al., 2007) and (4) fabrication of composite consisting of conducting polymers and substrates with high workability (Niwa et al., 1984; Paoli et al., 1984; Niwa et al., 1987; Yosomiya et al., 1986; Gregory et al., 1989; Heisey et al., 1993; Kuhn et al., 1995; Kincal et al., 1998; Appel et al., 1996; Collins et al., 1996; Kaynak et al., 2002; Han et al., 1999; Han et al., 2001; Dong et al., 2004; Dong et al., 2004; Abidian et al., 2006; Oh et al., 1999; Kim et al., 2002; Huang et al., 2005).

There have been numerous reports on the deposition of air-stable conducting organic polymers such as polypyrrole (PPy), polyaniline (PANI), or poly(3,4-ethylenedioxythiophene) (PEDOT) onto fibrous substrates (Gregory et al., 1989; Heisey et al., 1993; Kuhn et al., 1995; Kincal et al., 1998; Appel et al., 1996; Collins et al., 1996; Kaynak et al., 2002; Han et al., 1999; Han et al., 2001; Dong et al., 2004; Dong et al., 2004; Abidian et

al., 2006; Oh et al., 1999; Kim et al., 2002; Huang et al., 2005). The synthesis of conducting polymer-coated fibers has attracted much interest, due to the increasing applications of these fibers including microwave attenuation, static charge dissipation and electromagnetic interference shielding. Despite a significant amount of work on the synthesis and characterization of fibers coated with various conductive polymer shells and their corresponding hollow tubes, there is no report on conducting polymer-noble metal nanocomposite-coated fibers, to our best knowledge. The main benefit from the introduction of noble metal nanoparticles to fibrous surfaces is to avoid the spread of the nanoparticles to the environment. Conducting polymer-noble metal nanocomposites provide an exciting system to investigate the possibility of designing device functionality (Gangopadhyay et al., 2000) and also exhibit enhanced sensing and catalytic capabilities, compared with those of the pure conducting polymers (Tian et al., 1991; Drelinkiewicz et al., 2000; Kitani et al., 2001; Radford et al., 2001; Pillalamarri et al., 2005). The coating of such conducting polymer-metal nanocomposite on the substrates typically requires more than two steps including purification steps: (i) coating of the substrates with a conductive polymer and (ii) application of metal nanoparticles onto the conducting polymer shells.

Recently, it was reported that conducting polymer-noble metal nanocomposites can be synthesized by a one-step chemical oxidative polymerization using metal salts as an oxidant (Scheme 1) (Selvan et al., 1998; Chen et al., 2005; Chen et al., 2005; Fujii et al., 2007; Freund et al., 2001; Fujii et al., 2010; Vasilyeva et al., 2008; Fujii et al., 2010). It was demonstrated that chemical oxidative polymerization using metal salts such as hydrogen tetrachloroaurate(III), silver nitrate ($AgNO_3$), palladium(II) chloride ($PdCl_2$), and hydrogen hexachloroplatinate(IV) (H_2PtCl_6), which act both as an oxidant and as a source of metal atoms, yielded well-dispersed metal nanoparticles in/on bulk conducting polymers. Selvan *et al*. (Selvan et al., 1998) polymerized pyrrole with tetrachloroauric acid as an oxidant in the presence of polystyrene-*b*-poly(2-vinylpyridine) copolymer micelles dispersed in toluene, which led to the fabrication of PPy-Au nanocomposites. Chen *et al*. (Chen et al., 2005; Chen et al., 2005) and the present authors (Fujii et al., 2007) have demonstrated a one-step facile and versatile synthetic route to PPy-Ag nanocomposites by chemical oxidative polymerization using $AgNO_3$ as an oxidant in aqueous media. Henry *et al*. (Henry et al., 2001) and the present authors (Fujii et al., 2010) suggested that $PdCl_2$ acts as an efficient oxidant for pyrrole to form PPy-Pd composite in aqueous media (Scheme 1). More recently, Vasilyeva *et al*. (Vasilyeva et al., 2008) described the synthesis of PPy-Pd nanocomposites via direct redox reaction between Pd(II) acetate and pyrrole in acetonitrile. We have succeeded in one-step synthesis of PANI-Ag (Fujii et al., 2010) and PPy-Au (Fujii et al., 2008) nanocomposites by chemical oxidative polymerization in aqueous media.

In the present work, a facile and new chemical approach is developed to enable nanoprecise coating of conducting polymer-noble metal nanocomposite on fibers without disrupting their morphological hierarchies: we describe the one-step facile coating of fibers with conducting polymer-noble metal nanocomposites by chemical oxidative polymerization using metal salts in aqueous media (Scheme 2). To the authors' knowledge, this is the first report of a one-step and one-pot coating of fibrous substrates with conducting polymer-metal nanocomposites. The pristine fibers and resulting composite fibers were extensively characterized with respect to fiber diameter, morphology and surface/bulk chemical compositions by optical microscopy and scanning/transmission electron microscopies, elemental analysis, energy dispersive X-ray spectroscopy, X-ray photoelectron spectroscopy and X-ray diffraction, respectively. Diacetate, polyamide, silk, cotton, viscose, wool and

glass fibers were used as a substrate. The nanocomposite-coated fibers functioned as an efficient catalyst for Suzuki-type coupling reactions in aqueous media for the formation of carbon-carbon bonds.
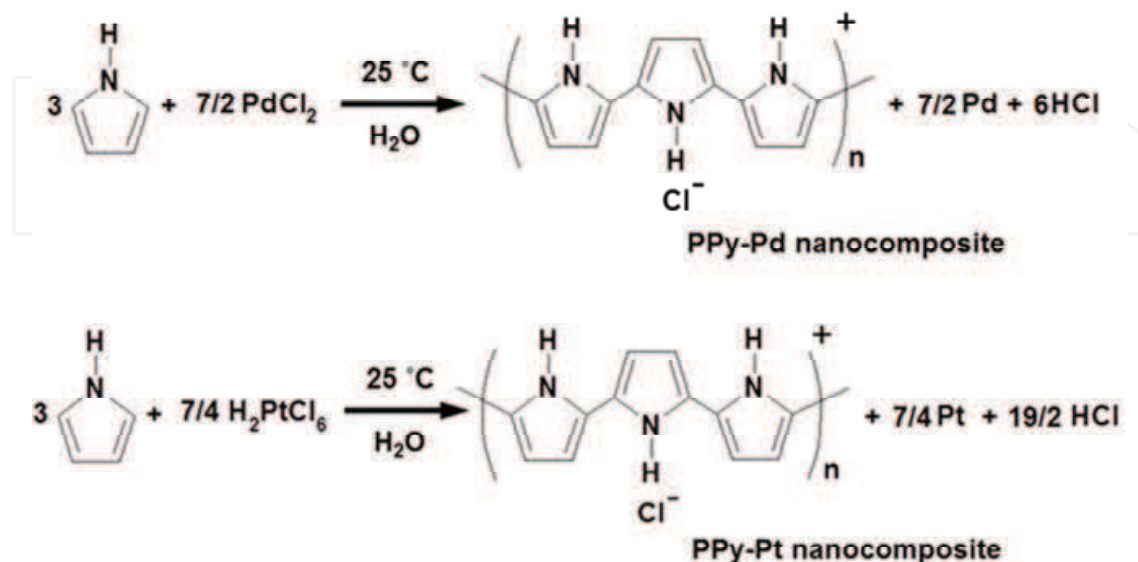
Scheme 1. Chemical oxidative polymerization of pyrrole using metal salts toward conducting polymer-metal nanocomposites.
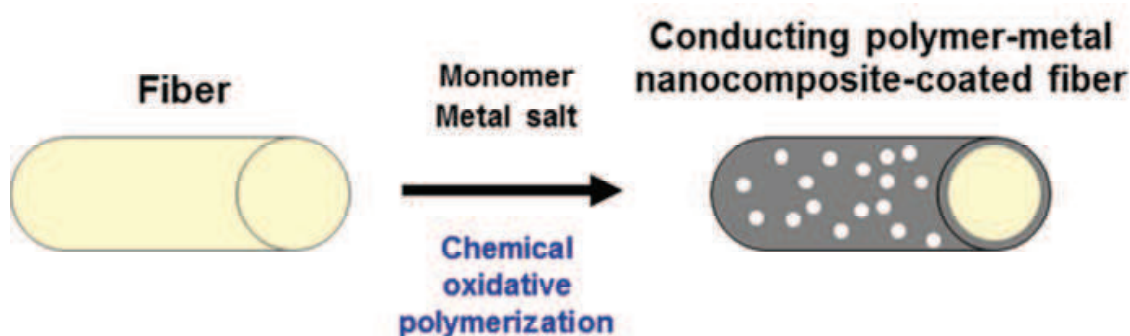
Scheme 2. One-step facile syntheses of fibers coated with conducting polymer-noble metal nanocomposites in aqueous media.

2. Experimental

2.1 Materials

Unless otherwise stated, all materials were guaranteed reagent grade. Palladium(II) chloride (PdCl$_2$, 99.9%), hydrogen hexachloroplatinate(IV) hexahydrate, (H$_2$PtCl$_6 \cdot$6H$_2$O, 99.9 %), dimethyl sulfoxide (DMSO, 99.9 %), p-methylphenylboronic acid (96%) and p-(trifluoromethyl)phenylboronic acid were obtained from Wako Chemicals. p-Bromotoluene (99%) and p-bromoanisole (97%) were obtained from Tokyo Chemical Industry Co., Japan. Sodium chloride (NaCl, 99.5%), hydrated ferric chloride (FeCl$_3$·6H$_2$O) and aluminium oxide (activated, basic, Brockmann 1, standard grade, ~150 mesh, 58 Å) were obtained from Sigma-Aldrich and were used without further purification. Pyrrole (Py, 98%) was also

obtained from Sigma-Aldrich and purified by passing through a column of the activated basic alumina prior to storage at –15 $^{\circ}$C before use. Deionized water (< 0.06 µS cm^{-1}) was prepared using a deionized water producing apparatus (Advantec MFS RFD240NA: GA25A-0715) and used for syntheses and purifications of the nanocomposite-coated fibers. Polymeric fibers (AATCC Multifiber Adjacent Fabric [Style #1, Lot #800, Piece #1886-26)]) were purchased from Testfabrics, Inc. (USA). The fiber samples were obtained as fabrics consisting of six kinds of polymeric fibers, namely spun diacetate, bleached cotton, spun polyamide (nylon 6,6), spun silk, spun viscose and worsted wool. As inorganic fibers, glass fibers were used: Quartz fiber filter (Lot No. 91210714, Grade QR-100, circles 21 mm) was purchased from Advantec®. Silica glass microfibre thimble (Cat No. 2812259, external diameter × external length 25 mm × 90 mm) was purchased from Whatman®. The fibers used in this study were used after washing using 2-propanol.

2.2 Synthesis of PPy and PPy-metal nanocomposite bulk powders

Chemical oxidative precipitation polymerization was conducted to obtain PPy-metal nanocomposites and PPy homopolymer bulk powders. The PPy-Pd nanocomposite bulk powder was synthesized as follows. PdCl$_2$ (0.154 g, 8.69×10^{-4} mol) and NaCl (0.102 g, 1.75×10^{-3} mol) were dissolved in deionized water (5.0 g) at 25 $^{\circ}$C. This aqueous solution was injected via syringe into a stirred pyrrole aqueous solution (1.0 wt%, 5.0 g: pyrrole, 7.45×10^{-4} mol). The solid-state density of the PPy-Pd nanocomposite bulk powder was measured to be 2.708 g/cm^3 by helium pycnometry using a Micromeritics Accu Pyc 1330 instrument. The PPy-Pt nanocomposite bulk powder was also synthesized using H$_2$PtCl$_6$·6H$_2$O in the same manner. The PPy homopolymer bulk powder was synthesized as follows. FeCl$_3$·6H$_2$O (0.470 g, 1.74×10^{-3} mol) was dissolved in deionized water (5.0 g) at 25 $^{\circ}$C. This aqueous solution was injected via syringe into the stirred pyrrole aqueous solution (1.0 wt%, 5.0 g: pyrrole, 7.45×10^{-4} mol). In all cases, the polymerization solutions were stirred (magnetic stirrer, 250 rpm) for 7 days at 25 $^{\circ}$C and the resulting black precipitates were washed several times with de-ionized water, followed by freeze-drying overnight.

2.3 Deposition of PPy-metal nanocomposite onto fibers

The following protocol was used for coating the fibers with a PPy-Pd nanocomposite overlayer at a pyrrole concentration of 100 wt% (based on the fibers). Pyrrole (0.01 g, 1.49 × 10^{-4} mol) was added by syringe to an aqueous media containing fiber (2.0 g, containing 0.01 g fiber) in a 13 mL screw-capped bottle and the system was left for 1 h with magnetic stirring. PdCl$_2$ oxidant (31 mg, 1.74×10^{-4} mol) and NaCl (31 mg, 5.22×10^{-4} mol) were dissolved in 1.0 g water and then added to the aqueous media containing the fiber. NaCl was added in order to dissolve PdCl$_2$ in the aqueous medium. The polymerization was allowed to proceed for 4 days at 300 rpm. Chemical oxidative polymerization of pyrrole proceeds with a reaction stoichiometry of 2.33 moles of electrons per mole of monomer (Armes et al., 1991). The Pd^{2+}/pyrrole molar ratio was adjusted to 1.17: two electrons are necessary to reduce one Pd(II) ion. In order to control the PPy-Pd nanocomposite loading on the fibers, the pyrrole concentration was systematically varied from 2 to 100 wt% with respect to the fiber. PPy-Pt nanocomposite coatings of fibers were also conducted by the chemical oxidative aqueous polymerization in the same manner using H$_2$PtCl$_6$·6H$_2$O as an oxidant; the ratio of pyrrole monomer and the weight of the fiber was adjusted to be the same with the 100 wt% system. The PPy-metal nanocomposite-coated fibers were subsequently purified by repeated ultrasonic cleaning in water (successive supernatants

were replaced with de-ionized water) in order to remove the unwanted inorganic by-products (water-soluble metal salts, NaCl and HCl).

2.4 Characterization of fibers and PPy-metal nanocomposite-coated fibers

Digital photography

Digital images were captured using a Ricoh Caplio R7 camera.

Optical microscopy

Fiber was placed on a microscope slide and observed using an optical microscope (Shimadzu Motic BA200) fitted with a digital system (Shimadzu Moticam 2000).

Transmission electron microscopy study

Examination of samples placed on carbon-coated copper grids was performed using a transmission electron microscope (TEM; Jeol JEM-2000EX).

Scanning electron microscopy study

Scanning electron microscopy (SEM; Keyence VE-8800, 12 kV) was conducted with Au sputter-coated (Elionix SC-701 Quick Coater) dried samples.

Energy dispersive X-ray spectroscopy study

Elemental analysis of the fibers was performed using a JSM-7001FA field emission scanning electron microscope equipped with an energy dispersive X-ray (EDX) microanalyzer operating at 15 kV.

Fourier transform infrared spectroscopy

The composition of the synthesized nanocomposite-coated fibers was studied using Fourier transform-infrared spectroscope (FT-IR; Horiba Freexact-II FT-720) with samples dispersed in KBr discs at 20 scans per spectrum with 4 cm^{-1} resolution.

Chemical composition

The PPy-metal nanocomposite and PPy loadings of the nanocomposite-coated fibers were determined by comparing the nitrogen contents determined by CHN elemental microanalysis (Yanaco CHN-Corder MT-5) with those of the PPy-metal and PPy bulk powders prepared by precipitation polymerization.

X-ray photoelectron spectroscopy study

For X-ray photoelectron spectroscopy (XPS) analyses, the dried powder samples were spread on an indium plate with a spatula and mounted onto sample stubs using conductive tape. XPS measurements were carried out using an XPS spectrometer (Axis Ultra) with a monochromated Al Kα X-ray gun. The base pressure was < 1.0×10^{-8} Torr. Pass energies of 80 eV and 20 eV were employed for the survey spectra and elemental core-line spectra, respectively. Quantification of the atomic percentage composition was obtained from high resolution spectra according to the manufacturer sensitivity factors. Spectra were aligned to the hydrocarbon component of the C 1s peak set at 285 eV.

X-ray diffraction measurement

Powder X-ray diffraction analysis of air-dried samples was performed with an X-ray diffractometer (XRD; Rigaku RINT 2200) using Ni-filtered Cu Kα (1.54056 Å) radiation.

Conductivity measurements

The electrical conductivity of the dried samples was determined for pressed pellets (13 mm diameter, prepared at 300 kg cm^{-2} for 16 min) at room temperature using a conventional four-point-probe technique with a resistivity meter (Loresta-GP MCP-T610, Mitsubishi Chemical Co.).

Contact angle measurements

Contact angles for water droplets (10 μL) placed on pressed pellets prepared from dried PPy-Pd nanocomposite bulk powder, wool fiber and PPy-Pd nanocomposite-coated wool fiber (pelletized at 300 kgcm^{-2} for 10 min using Shimadzu SSP-IOA hand press) were determined using an Excimer Simage02 apparatus at 25 °C.

2.5 Suzuki reaction in aqueous media using PPy-Pd nanocompoisite-coated fibers as a catalyst

A typical procedure is given for the reaction of bromobenzene with *p*-methylphenylboronic acid. To a screw-capped vial with a stirring bar were added 0.5 mmol of bromobenzene, 0.75 mmol of *p*-methylphenylboronic acid, PPy-Pd nanocomposite-coated polyamide fiber (6.4 mg, 0.10 mol% of Pd), and 1.5 mol L^{-1} aqueous potassium carbonate solution (1 mL). After stirring at 80 °C for 3 h, the reaction mixture was cooled to room temperature by immersing the vial in water (~20 °C). Subsequently, the aqueous phase was removed and the recovered catalyst was washed with water (5×1.5 mL) and diethyl ether (5×1.5 mL), which were then added to the aqueous phase. The aqueous phase was extracted five times with diethyl ether. The combined organic extracts were dried over MgSO$_4$, concentrated under reduced pressure, and purified by flash column chromatography on silica gel to give the desired product. The product was analyzed by ^{1}H NMR. ^{1}H NMR spectra in CDCl$_3$ were recorded with a 300 MHz NMR spectrometer (UNITY 300, Varian, Palo Alto, CA) using tetramethylsilane (δ = 0) as an internal standard. The same protocol was used for other Suzuki coupling reactions: the *p*-bromoacetophenone and *p*-methylphenylboronic acid system, the *p*-bromoanisole and *p*-methylphenylboronic acid system, and the *p*-bromotoluene and *p*-(trifluoromethyl)phenylboronic acid system.

3. Results and discussion

3.1 Characterization of fibrous substrates

The color of pristine polymeric fibers is white, because of light scattering at their surface. Optical microscopy and SEM studies indicated that diacetate, cotton and viscose fibers have 'flat-noodle' morphology: the diacetate fibers had wrinkles on their surfaces and the cotton fibers were twisted. Typical SEM images of the pristine fibers are shown in Figure 1. Diacetate fibers have number-average long-axis length of 27.9 ± 1.8 μm and short-axis length of 13.1 ± 2.2 μm. Cotton fibers have number-average long-axis length of 20.1 ± 3.2 μm and short-axis length of 6.5 ± 1.0 μm. Viscose fibers have number-average long-axis length of 18.8 ± 1.9 μm and short-axis length of 7.6 ± 0.9 μm. Polyamide, silk and wool fibers have cylindrical morphology. The number-average diameters of polyamide, silk and wool fibers were measured as 19.0 ± 1.1 μm, 11.7 ± 0.7 μm and 20.7 ± 3.0 μm, respectively (over 50 fibers were counted). On the surface of the wool fiber, cuticles were observed and a number-average height of the cuticle and a number-average distance between them were measured to be 830 nm and 9.74 μm, respectively. All the inorganic fibers used in this study are white

	Nitrogen content (CHN%) / wt%	PPy-Pd loading (CHN %) [a] / wt%	PPy loading (CHN %) [b] / wt%	Pd loading [c] / wt%	Shell thickness [d] / nm	Conductivity of pellet[e] / Scm^{-1}
Diacetate fiber	~0	-	-	-	-	< 10^{-8}
Cotton fiber	~0	-	-	-	-	< 10^{-8}
Polyamide fiber	11.92	-	-	-	-	< 10^{-8}
Silk fiber	~0	-	-	-	-	< 10^{-8}
Viscose fiber	24.33	-	-	-	-	< 10^{-8}
Wool fiber	15.25	-	-	-	-	< 10^{-8}
PPy-Pd bulk powder	6.36	100	38.6	61.4	-	3.0 × 10^{1}
PPy bulk powder	16.49	-	100	-	-	4.7 × 10^{0}
Diacetate/PPy-Pd (Py, 100 wt%)	0.27	4.3	1.7	2.6	98	3.1 × 10^{-6}
Diacetate/PPy-Pd (Py, 20 wt%)	0.22	3.5	1.4	2.1	79	< 10^{-8}
Diacetate/PPy-Pd (Py, 10 wt%)	< 0.22	< 3.5	< 1.4	< 2.1	< 79	< 10^{-8}
Diacetate/PPy-Pd (Py, 5 wt%)	< 0.22	< 3.5	< 1.4	< 2.1	< 79	< 10^{-8}
Diacetate/PPy-Pd (Py, 2 wt%)	< 0.22	< 3.5	< 1.4	< 2.1	< 79	< 10^{-8}
Cotton/PPy-Pd (Py, 100 wt%)	0.33	5.2	2.0	3.2	78	9.0× 10^{-5}
Polyamide/Ppy-Pd (Py, 100 wt%)	11.39	n.d.	n.d.	n.d.	n.d.	1.8× 10^{-5}
Silk/PPy-Pd (Py, 100 wt%)	0.22	3.5	1.4	2.1	55	6.0× 10^{-6}
Viscose/PPy-Pd (Py, 100 wt%)	23.91	n.d.	n.d.	n.d.	n.d.	7.4× 10^{-6}
Wool/PPy-Pd (Py, 100 wt%)	13.30	n.d.	n.d.	n.d.	n.d.	2.2× 10^{-6}

[a] Percentage mass of PPy-Pd nanocomposite loading on the fibers, as determined by nitrogen microanalyses (comparing to a nitrogen content of 6.36 % for PPy-Pd nanocompoisite bulk powder).

[b] Percentage mass of PPy component loading on the fibers, as determined by nitrogen microanalysis (comparing to a nitrogen content of 16.49 % for PPy bulk powder).

[c] Calculated using the following equation: PPy-Pd loading (CHN %) – PPy loading (CHN %).

[d] Calculated assuming the smooth shell using PPy-Pd nanocomposite loading (CHN %) and densities of fibers and PPy-Pd nanocomposite (2.708 gcm^{-3})

[e] Pressed pellet conductivity at 25 °C determined using the conventional four-point probe technique.

Table 1. Summary of microanalytical data, PPy-Pd nanocomposite, PPy and Pd loadings, shell thickness and conductivities of the uncoated polymeric fibers and PPy-Pd nanocomposite-coated polymeric fibers.
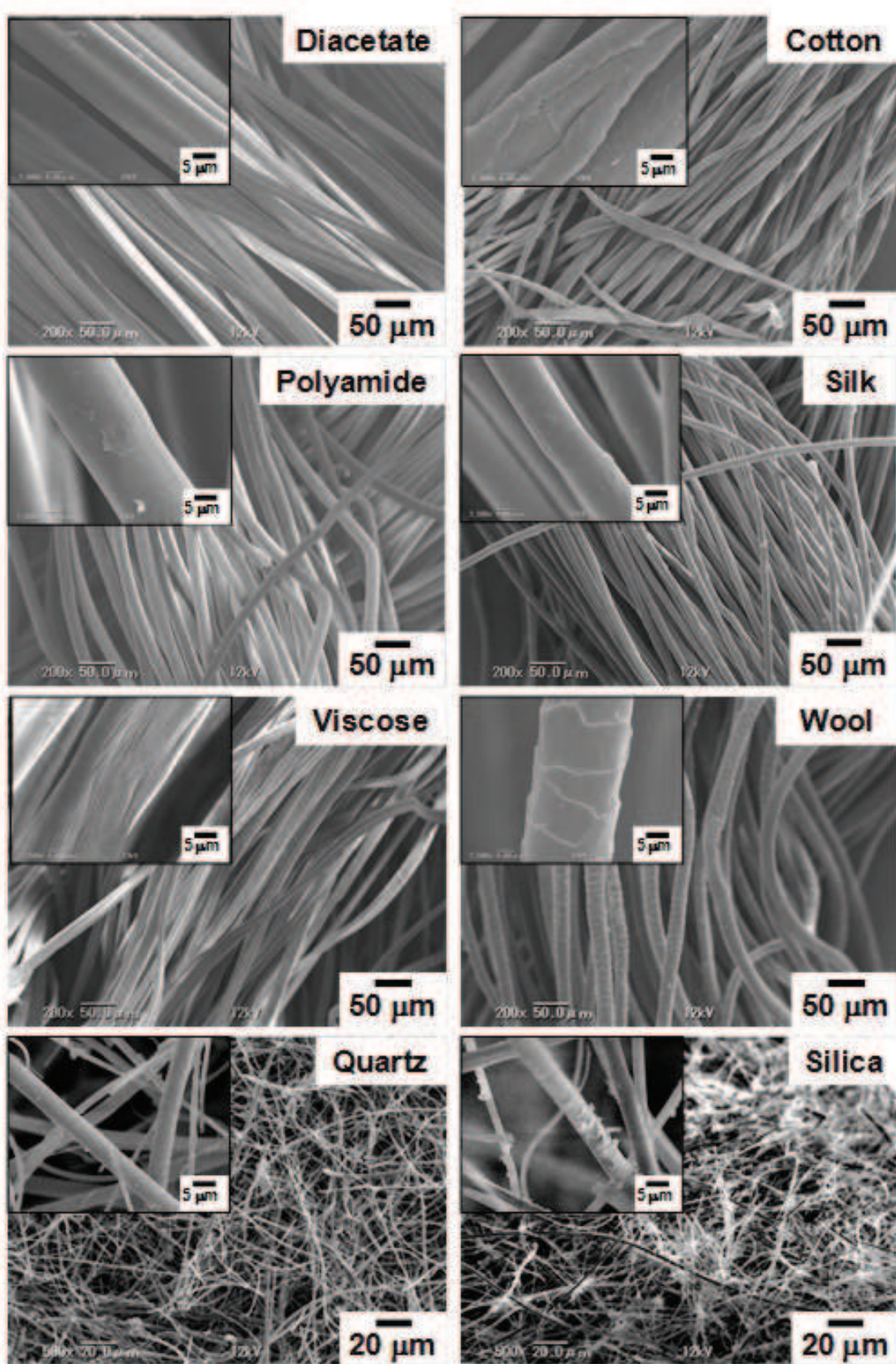
Fig. 1. SEM images of polymeric and inorganic fibers used in this study.

colored and have cylindrical morphology, which was confirmed by optical and SEM studies (Figure 1). The number-average diameters of the inorganic fibers were measured to be 1.2 ± 0.5 μm (Quartz Fiber Filter) and 0.8 ± 0.2 μm (Silica Glass Microfibre Thimbles) using the SEM images, respectively. Optical microscopy analyses confirmed that all the polymeric and inorganic fibers are well wetted with water and no bubble (larger than submicrometer) can be observed on their surfaces in aqueous media.

3.2 Conducting polymer-noble metal nanocomposite-coated fibers
3.2.1 Conducting polymer-metal nanocomposite coating on polymeric fibers

3.2.1.1 PPy-Pd nanocomposite-coated polymeric fibers

After addition of the $PdCl_2$ oxidant to the aqueous media containing polymeric fibers with dissolved pyrrole monomer, the polymerization system turned black within 10 min, which indicates the production of the PPy-Pd component. The color of the fibers changed from white to black, which suggests a deposition of black colored PPy-Pd nanocomposite on the fibers. The morphology of the synthesized fibers was assessed by optical microscopy. Optical microscopy indicated no signs of appreciable destruction of fibrous morphologies in all systems. SEM studies revealed that micrometer-sized fibers with surface nuclei ranging between 50 and 250 nm were obtained after chemical oxidative polymerization in all fiber systems (see Figure 2 inset). The nuclei on the surface seem to be due to the precipitation of PPy-Pd nanocomposite nuclei from the aqueous medium, which are then adsorbed by the fiber surfaces. Similar nuclei on the surface of the polymeric substrate were also observed in the case of PPy-Pd nanocomposite-coated polystyrene particles (Fujii et al., 2010). The pyrrole monomer was expected to polymerize exclusively in aqueous solution and/or on the fiber surface, because the ionic Pd^{2+} oxidant should not diffuse into the hydrophobic polymeric fibers; therefore, pyrrole polymerization within the fiber interior was highly unlikely. PPy-Pd nanocomposite component precipitated in the aqueous media and on the fiber surface should accumulate on the fiber surface in order to minimize interfacial free energy (Lovell et al., 1997; Okubo et al., 1999) and PPy-Pd nanocomposite-coated fibers with core-shell morphologies were expected.

A summary of the microanalytical data, PPy-Pd nanocomposite, PPy and Pd loadings, shell thickness and electrical conductivity of the uncoated fibers and the PPy-Pd nanocomposite-coated fibers is given in Table 1. Microanalytical studies indicate the PPy-Pd nanocomposite bulk powder consists of 38.6 wt% PPy and 61.4 wt% Pd components, which is in good agreement with the theoretical values calculated using the reaction scheme shown in Scheme 1 (PPy, 38.3 wt% and Pd, 61.7 wt%). This result indicates that the pyrrole was quantitatively polymerized with the Pd^{2+} oxidant. The percentage mass of the PPy-Pd nanocomposite loading on the composite fiber was determined by comparing the nitrogen content to that of the PPy-Pd composite bulk powder (N = 6.36%) synthesized in the absence of fibers. The percentage mass of the PPy component loading was also calculated by comparing the nitrogen content to that of chlorine-doped PPy homopolymer bulk powder prepared by chemical oxidative precipitation polymerization using $FeCl_3$ oxidant, assuming that the PPy component in the PPy-Pd nanocomposite and the PPy homopolymer have the same chemical structure. The PPy-Pd nanocomopsite loadings (Py, 100 wt% systems) were measured to be ranging between 3.5 and 5.2 wt% and there was no large difference.
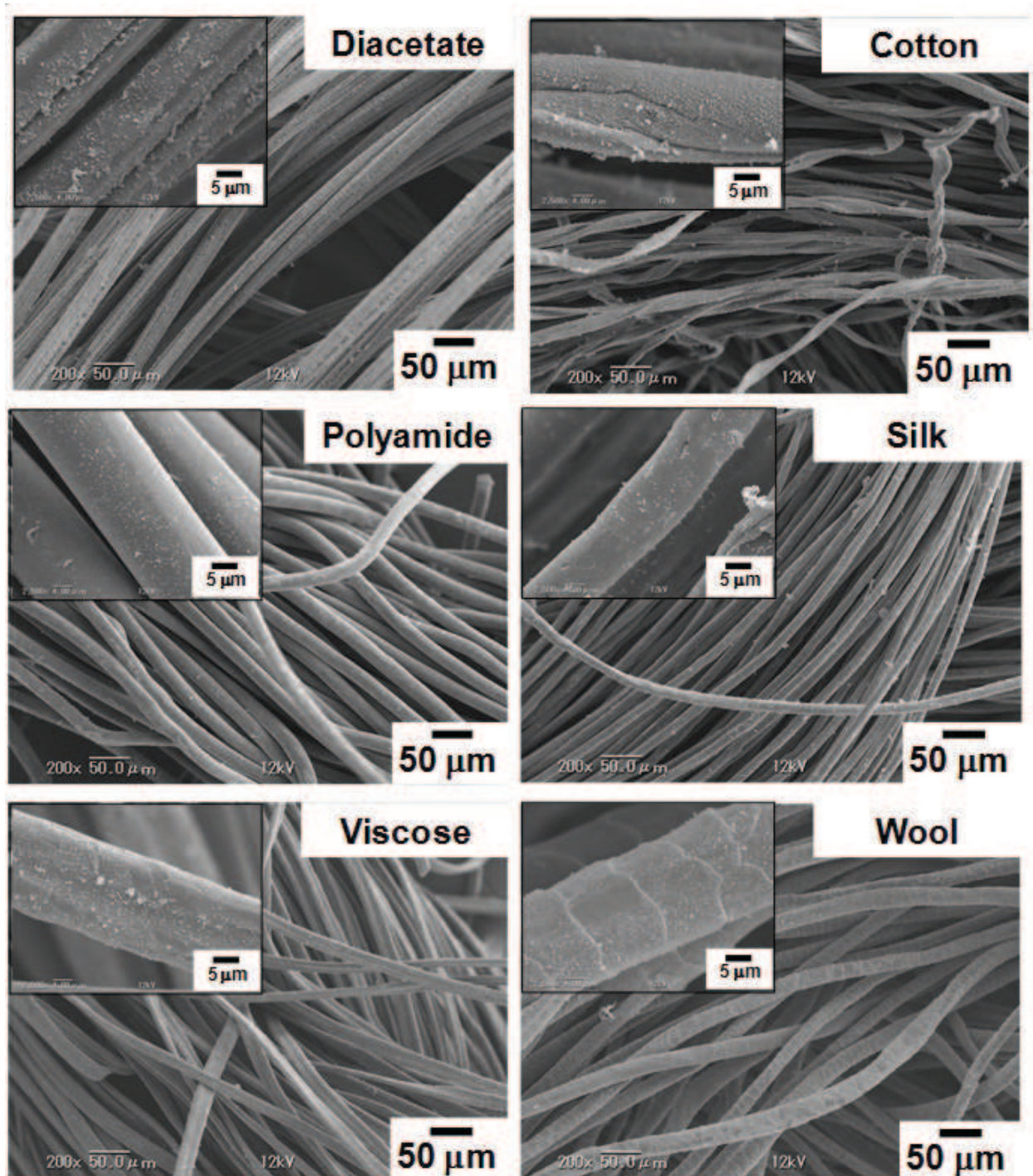
Fig. 2. SEM images of PPy-Pd nanocomposite-coated polymeric fibers (Py, 100 wt % based on fiber).

Considering that all the fibers have the similar diameters and specific surface areas, it is reasonable for the fibers to have the similar PPy-Pd nanocomposite loadings. These results also indicate the surface chemistry does not have a large effect on the PPy-Pd nanocomposite loading amount. The weight ratios of the PPy and Pd components in the nanocomposite-coated fibers were calculated to be around 39:61 for all the systems, which is again in good agreement with the theoretical values. These results indicate that the

polymeric fibers do not interfere with the chemical oxidative polymerization of pyrrole using Pd^{2+}.

The conductivities of pressed pellets of the PPy-Pd nanocomposite-coated fibers (Py, 100 wt% system) were measured to be in the order of $10^{-5} \sim 10^{-6}$ Scm^{-1} (Table 1), which are higher than those of the pristine fibers ($<10^{-8}$ Scm^{-1}). Although the conductivities of the PPy-Pd nanocomposite-coated fibers are relatively low, it is worth emphasizing that pressed pellets prepared from a heterogeneous admixture of 95 wt% polymeric fibers and 5 wt% PPy-Pd nanocomposite bulk powder had even lower electrical conductivity, which was below the lower limit for the four-point-probe set-up ($<10^{-8}$ S cm^{-1}). More efficient electrical conduction occurs in the PPy-Pd nanocomposite-coated fibers, because the electrons can flow with lower resistance between adjacent fibers via the conductive pathway provided by the PPy-Pd overlayers, without interference from the underlying electrically insulating fibrous cores. This result indicates that the composite fibers have lower percolation threshold comparing with the heterogeneous mixture of the polymeric fibers with PPy-Pd nanocomposite bulk powder. The same mechanism was also proposed in the conducting polymer-coated latex particles (Fujii et al., 2010; Lascelles et al., 1997; Okubo et al., 2001).
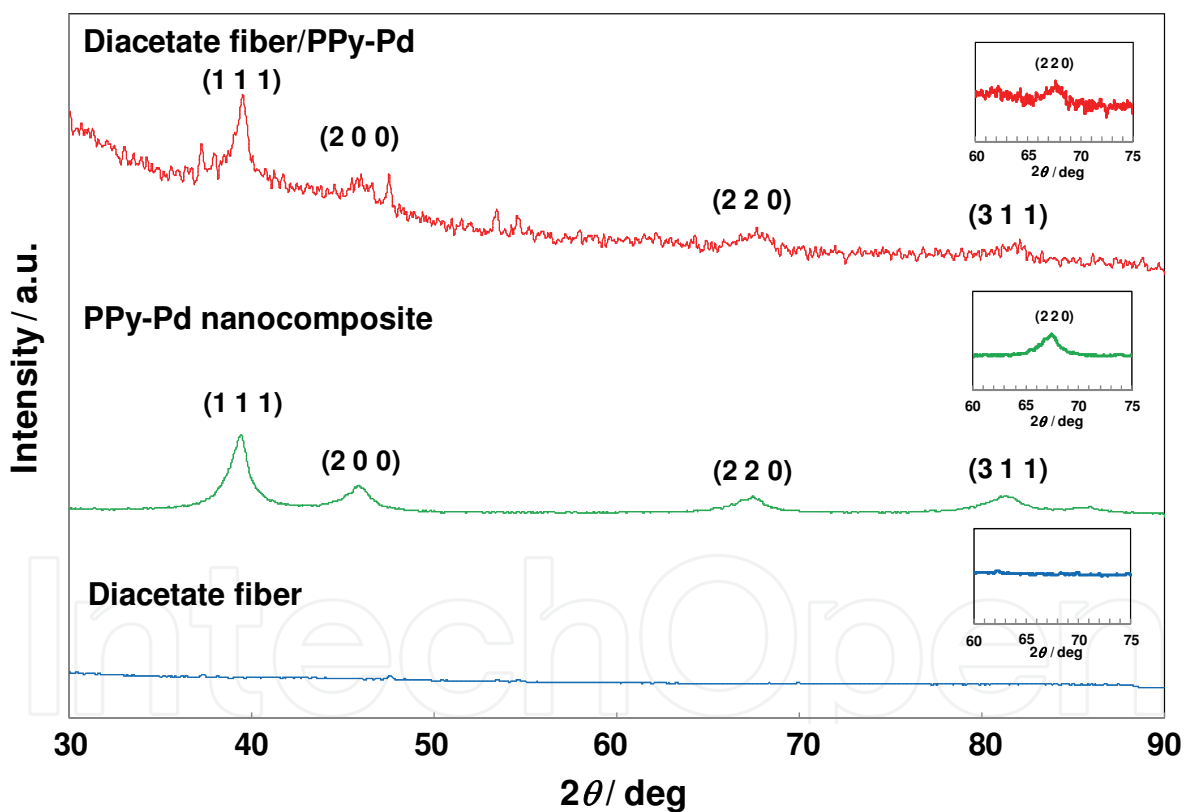

Fig. 3. XRD spectra obtained for PPy-Pd nanocomposite-coated diacetate fiber, PPy-Pd nanocomposite bulk powder and diacetate fiber.

FT-IR studies were conducted for the PPy-Pd nanocomposite-coated diacetate fibers (pyrrole 100 wt% system), the PPy-Pd nanocomposite bulk powder (synthesized by aqueous precipitation polymerization in the absence of polymeric fiber) and the uncoated diacetate fibers. The spectrum for the uncoated diacetate fibers shows the characteristic absorbances of carbonyl group at 1766 cm^{-1} and hydroxyl group in a range between 3100 and 3700 cm^{-1}.

The FT-IR spectrum of the PPy-Pd nanocomposite bulk powder, which shows characteristic bipolaron bands at 1196 and 934 cm^{-1} and broad bands at 1538 and 1043 cm^{-1}, indicates the formation of PPy in its doped state (Bjorklund et al., 1986). The spectrum for the PPy-Pd nanocomposite-coated diacetate fibers is very similar to that obtained for the pristine diacetate fibers. This is not particularly surprising, given that these composite fibers comprise more than 96% diacetate by mass and the diacetate component dominates the FT-IR spectrum.

In order to confirm the presence of a Pd component in the composite fibers, XRD studies were carried out. XRD patterns of the PPy-Pd nanocomposite-coated diacetate fibers (pyrrole 100 wt%), the PPy-Pd nanocomposite bulk powder and the diacetate fibers are shown in Figure 3. Four peaks at 39.5°, 45.1°, 67.4° and 82.1° 2θ, which correspond to the (111), (200), (220) and (311) lattice plane diffractions of Pd crystals, are clearly observed for the PPy-Pd nanocomposite-coated diacetate fibers and the PPy-Pd nanocomposite bulk powder. These peaks are in agreement with those reported for Pd nanoparticles (Zhang et al., 2008; Wen et al., 2008). There are no detectable peaks due to PdCl$_2$ (*e.g.* 16.7°, 28.7°, 37.6° and 56.0° 2θ), which provides unambiguous evidence that the reduction of Pd(II) to Pd(0) has taken place. On the other hand, only a very broad peak was observed at 18° for the amorphous diacetate fiber (data not shown).

In order to confirm the presence of Pd and PPy components on the fiber surface (~ 10 nm), XPS studies were carried out. Figure 4 shows the XPS survey spectra of the PPy-Pd nanocomposite-coated diacetate fibers (pyrrole 100 wt% system), the PPy-Pd nanocomposite bulk powder and the diacetate fibers. Signals due to Pd and N, in addition to those due to C and O, are clearly apparent for the PPy-Pd bulk powder and the PPy-Pd nanocomposite-coated diacetate fiber, which indicates the existence of PPy and Pd components on the fiber surface. Pd percentages on the surface were calculated to be 4.97 mol% and 6.39 mol% for the PPy-Pd nanocomposite-coated diacetate fiber and the bulk powder, respectively. The O 1s signal observed in the nanocomposite bulk powder spectrum should arise from the partial over-oxidation of the PPy backbone. A signal due to Cl 2p was also observed in the PPy-Pd nanocomposite bulk powder spectrum, which indicates that the cationic PPy chains are doped with chloride anions (from the PdCl$_2$ oxidant and NaCl): it was difficult to observe the Cl 2p signal in the PPy-Pd nanocomposite-coated fibers in the survey spectrum, but it can be detected in narrow scan spectrum. The Cl/N atomic ratios of the PPy-Pd bulk powder and the composite fibers were estimated from the XPS spectra to be 0.34 and 0.036 respectively. The Cl/N atomic ratio for the bulk powder accords well with that calculated based on the chemical structure shown in Scheme 1 (0.33). The lower Cl/N atomic ratio for the composite fibers might be due to the likelihood of surface degradation and concominant loss of Cl dopant. The surface C/N atomic ratio of the PPy-Pd nanocomposite-coated diacetate was determined to be 3.13, which accords with that of the PPy-Pd nanocomposite bulk powder (3.29). These C/N ratios are in good agreement with the theoretical value calculated for PPy component (3.33). From the XPS results, it has been confirmed that the PPy-Pd nanocomposite coated the polymeric fiber substrates.

To map Pd element on synthesized composite diacetate fibers, EDX study was conducted. EDX image for Pd element of the PPy-Pd nanocomposite-coated diacetate fibers is depicted in Figure 5. The EDX image of the composite fibers revealed that Pd element existed homogeneously on the surface of PPy-Pd nanocomposite-coated diacetate fibers.
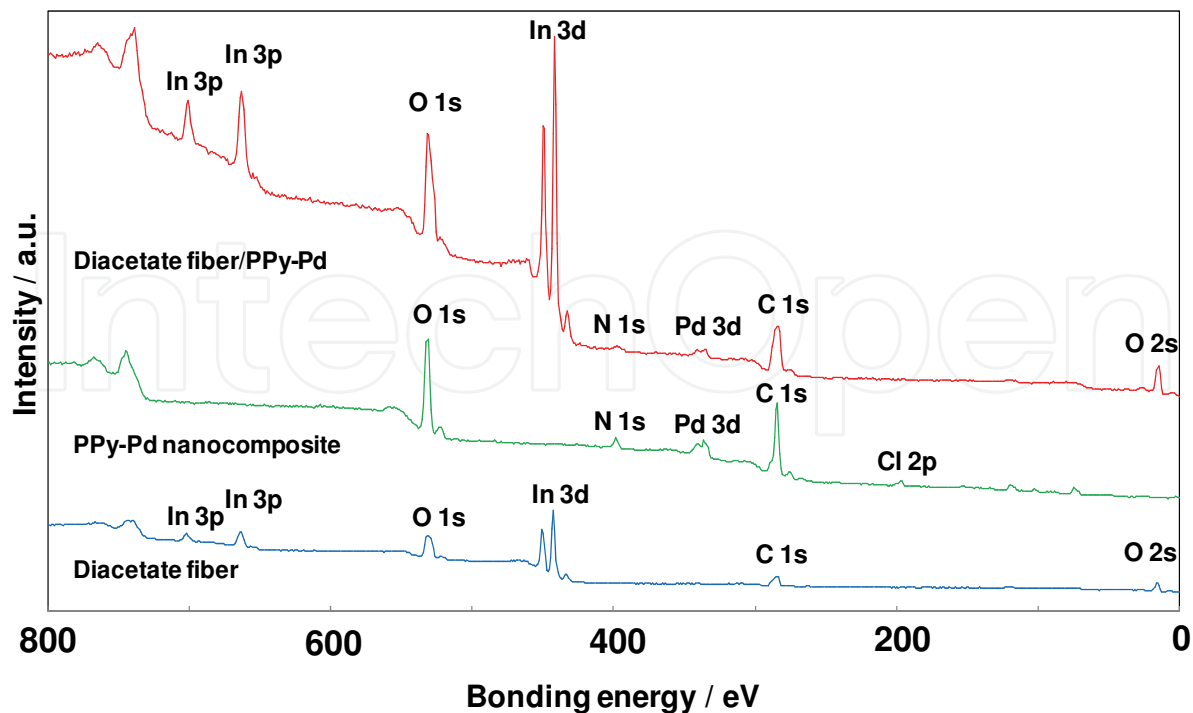
Fig. 4. XPS survey spectra obtained for PPy-Pd nanocomposite-coated diacetate fiber, PPy-Pd nanocomposite bulk powder and diacetate fiber.
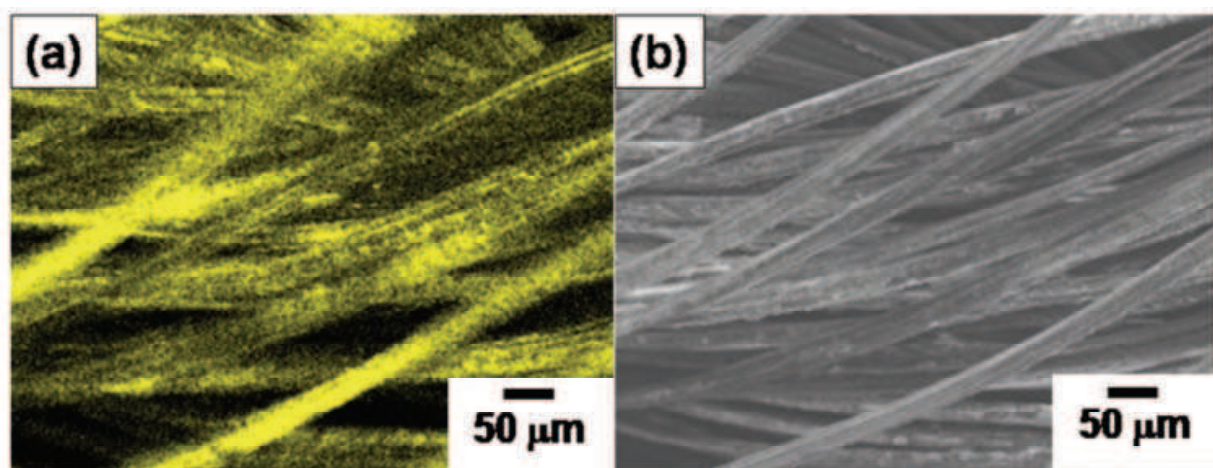

Fig. 5. (a) EDX image for Pd element and (b) SEM image of PPy-Pd nanocomposite-coated diacetate fiber.

Surface coating with PPy-Pd nanocomposite can also be confirmed by contact angle measurement studies. Contact angle measurement is an established technique for investigating surface hydrophilic/hydrophobic characters. The static contact angle for a sessile water drop on a pressed pellet of the fibers was measured. The contact angles for the pristine wool fibers and the PPy-Pd nanocomposite bulk powder were measured to be 141° and 60°, respectively. The contact angle for the PPy-Pd nanocmopsote-coated wool fibers was 121°, which sits between the two contact angle values. This result can be explained by the PPy-Pd nanocomposite coating on the wool fibers, which will increase the hydrophilic character for the fiber surface.

The core-shell nature of the PPy-Pd nanocomposite-coated fibers has been readily verified by solvent extraction of the fiber core, followed by morphological examination of the insoluble PPy-Pd residues. DMSO was used for the extraction of diacetate and viscose fibers. Hot KOH aqueous solution (80 °C) and formic acid were used for the extraction of wool and polyamide fibers, respectively. Extraction of core component from the composite fibers using the solvents resulted in insoluble black residues: the composite fibers were dispersed in solvents for 24 h and were washed by replacing the solvents (five cycles) with pure solvents. Analysis of the black residues by FT-IR spectroscopy and CHN elemental microanalysis confirmed that these material were PPy-Pd nanocomposite and contained little core components. These results indicate that almost the core component was extracted from the original composite fibers. Examination of the black PPy-Pd nanocomposite residues by optical microscope revealed 'tubular' morphologies, with diameters corresponding to those of the original coated fibers (Figure 6). The solvent extraction experiment confirms that the composite fibers do possess a core-shell morphology, which is consistent with the XPS, EDX and contact angle results. Shell thicknesses were calculated to be ranging between 55 and 98 nm assuming the smooth shell surface using PPy-Pd nanocomposite loading% and densities of fibers and PPy-Pd nanocomposite (Table 1). The structure of PPy-Pd nanocomposite shell (pyrrole 100 wt%) was investigated using a TEM in detail (Figure 7). The TEM images revealed that there are two Pd size distributions in diacetate, polyamide and viscose systems (approximately 6 nm and 1.4 nm). The 6-nm Pd nanoparticles formed aggregates (50~250 nm), which were observed in bump-like projections on a fiber surface. Heterogeneous character of the continuous shell was composed of a more transparent host material (presumably the PPy polymer) with incorporated 1.4 nm-sized Pd nanoparticles that have a higher absorbance for TEM electrons (dark elements dispersed in the PPy matrix.). The mechanism resulting in these two Pd size distributions (6 nm and 1.4 nm) is not clear at this stage, and we are currently exploring the effect of the polymerization conditions on the Pd nanoparticle size distribution. An interesting characteristic of the conducting polymer tubes is that the transport rates of small molecules into the tube core are affected by the oxidation state of the conductive polymer (Abidian et al., 2006), a feature with potential application in many molecular uptake and release scenarios. The PPy-Pd nanocomposite loading was simply controlled by varying the amount of pyrrole monomer based on the fibrous substrates in the polymerization recipe: an increase of the pyrrole/diacetate fiber ratio increased the PPy-Pd nanocomposite loading. The chemical oxidative polymerization was conducted in the presence of diacetate fibers at various Py concentrations (2~20 wt% based on the fibers). As the fiber surface area available for PPy-Pd nanocomposite deposition was increased, the amount of free by-product PPy-Pd nuclei decreased. In all systems, micrometer-sized fibers with surface nuclei ranging between 50 and 250 nm were obtained after chemical oxidative polymerizations. The PPy-Pd loadings were lower than the theoretical values calculated from the polymerization reactions. The lower PPy-Pd loadings are due to the removal of free PPy-Pd by-products by washing with aqueous media prior to elemental analysis. Examination of the black PPy-Pd nanocomposite residues obtained after the extraction of diacetate from the composite fibers by optical microscope revealed 'tubular' morphology, with a diameter corresponding to that of the original composite fibers, at 20 wt% system (Figure 8). In the cases of the 10, 5 and 2 wt% systems, the PPy-Pd nanocomposite coating was relatively inhomogeneous, due to low PPy-Pd nanocomposite loadings, so that the shell cannot maintain complete tubular morphology and was partially broken. In these systems, two Pd nanoparticle size
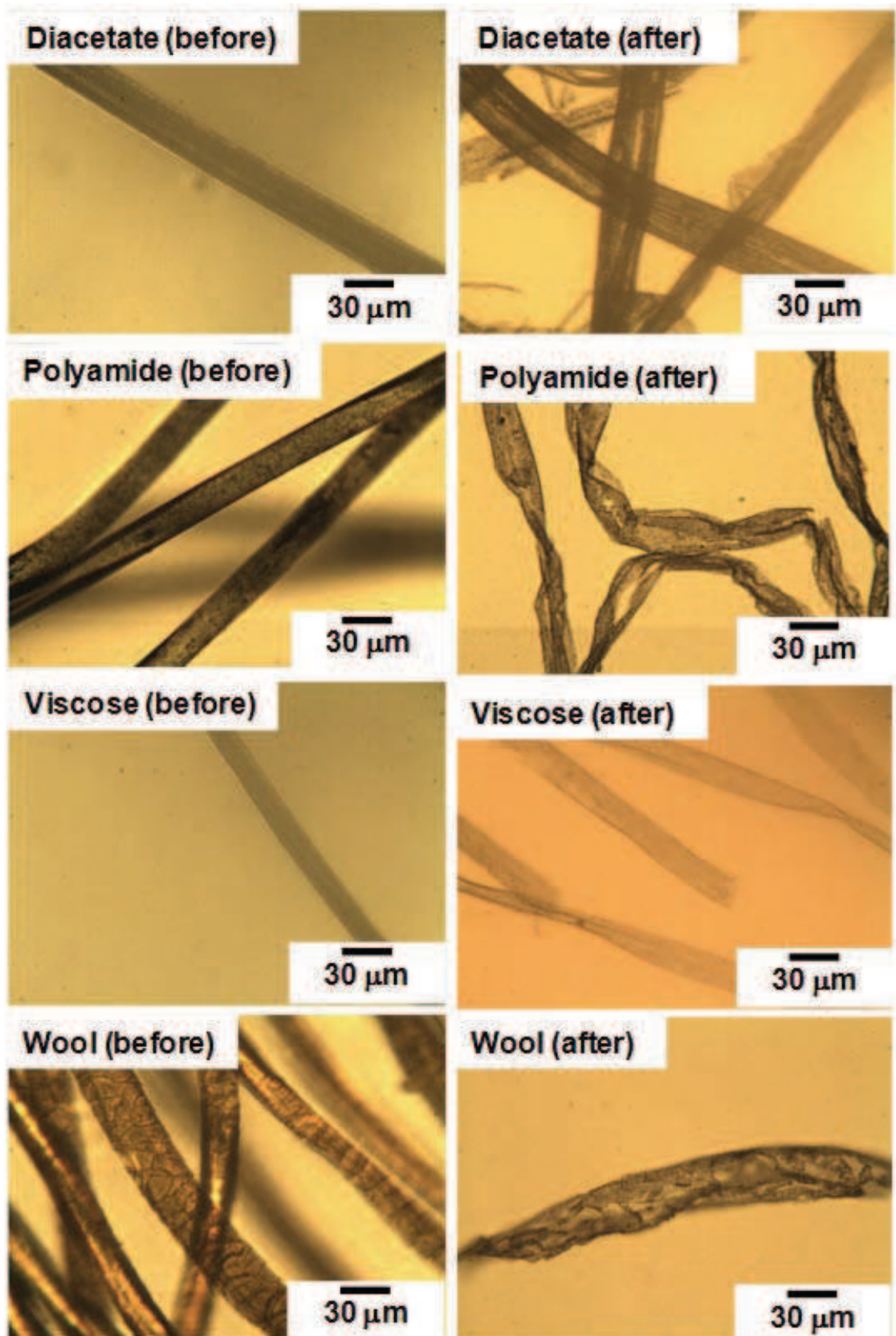
Fig. 6. Optical micrographs of PPy-Pd nanocomposite-coated polymeric fibers before and after extraction of fibers.
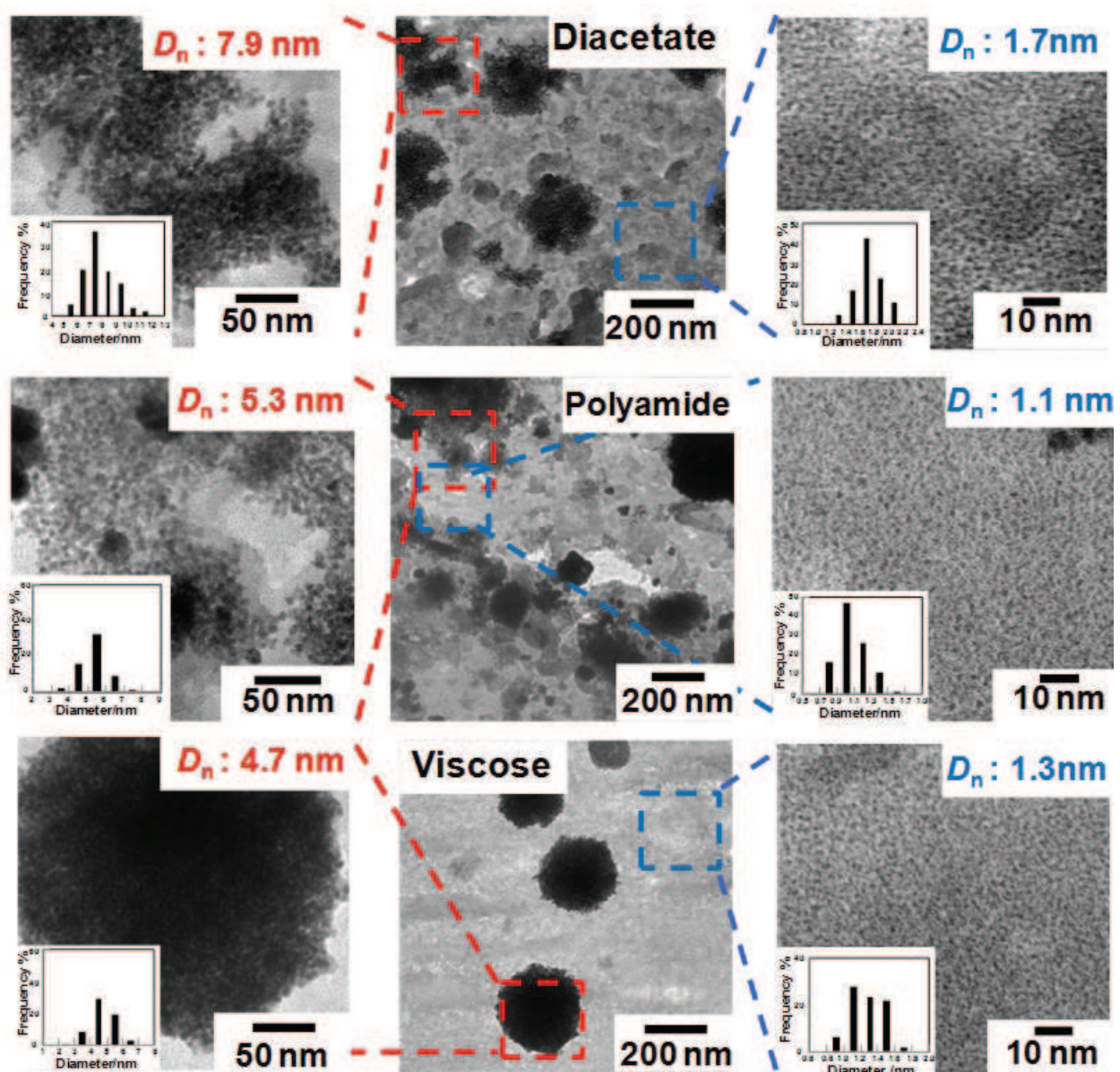
Fig. 7. TEM images of PPy-Pd nanocomposite-coated fibers after extraction of fibers. DMSO (for diacetate and viscose) and formic acid (for polyamide) were used for extraction of polymeric fibers.

distributions were again observed by TEM. Unfortunately, the conductivity was measured to be below 10^{-8} S cm^{-1}, which is lower measurable limit by our four-point-probe set-up, for PPy-Pd nanocomposite-coated diacetate fibers synthesized at Py concentrations of 20, 10, 5 and 2 wt%.

Finally, the deposition of PPy-Pd nanocomposite in a large scale was investigated. Nanocomposite coating can be conducted on woven cloth which consists of fibers, such as a T-shirt. Figure 9 shows digital camera images of a T-shirt before and after PPy-Pd nanocomposite coating by chemical oxidative polymerization in aqueous media at room temperature. In this system, Py concentration was set at 1.0 wt% based on the T-shirt. The color of the T-shirt changed from white to black after the chemical oxidative polymerization, which indicates the nanocomposite coating. The color of the T-shirt was not breached even

after five times sonication in aqueous media, which indicated that the fibers were firmly coated with the PPy-Pd nanocomposite. This synthetic route is advantageous because the reaction takes place in aqueous media at room temperature and production on an industrial scale is much more likely compared to a two-step synthetic route.
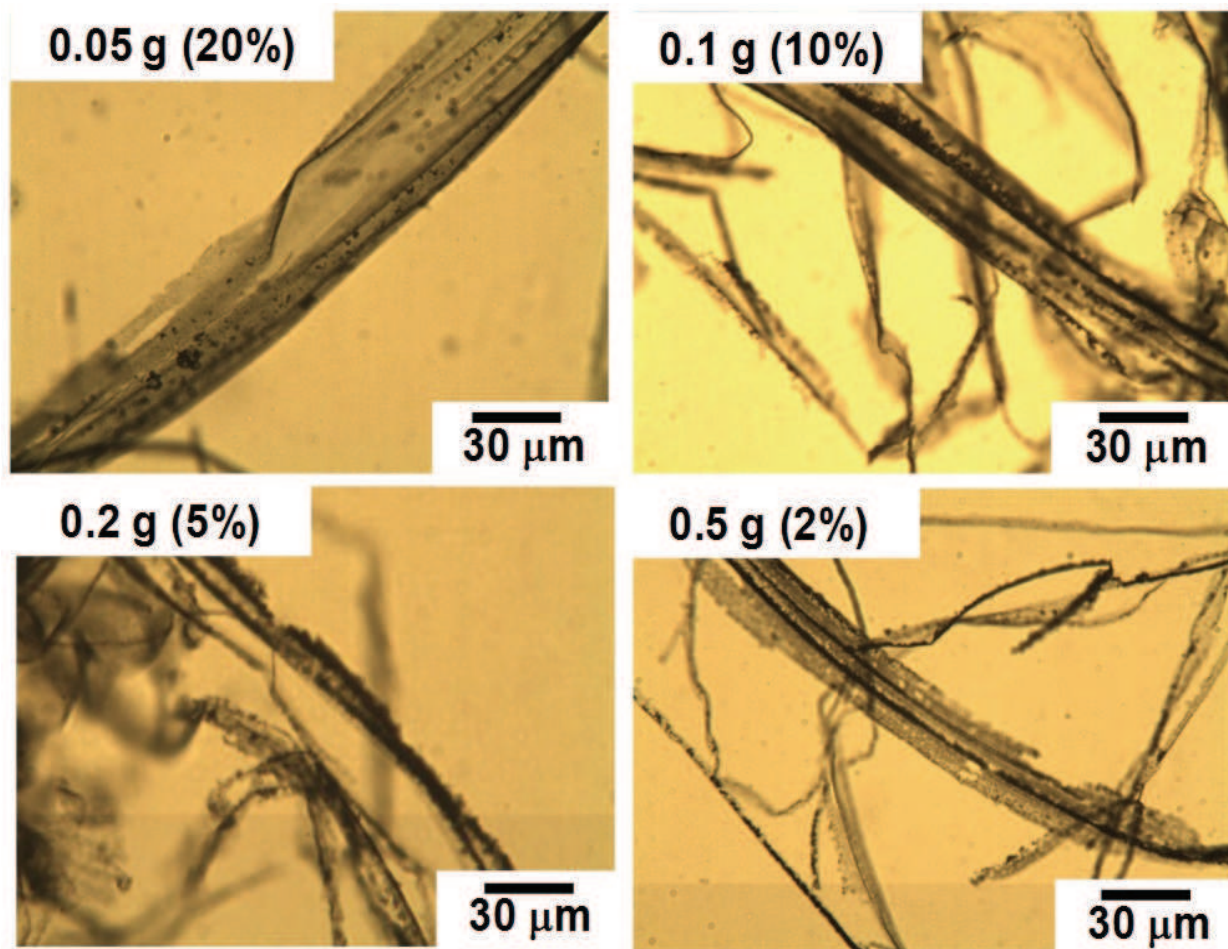

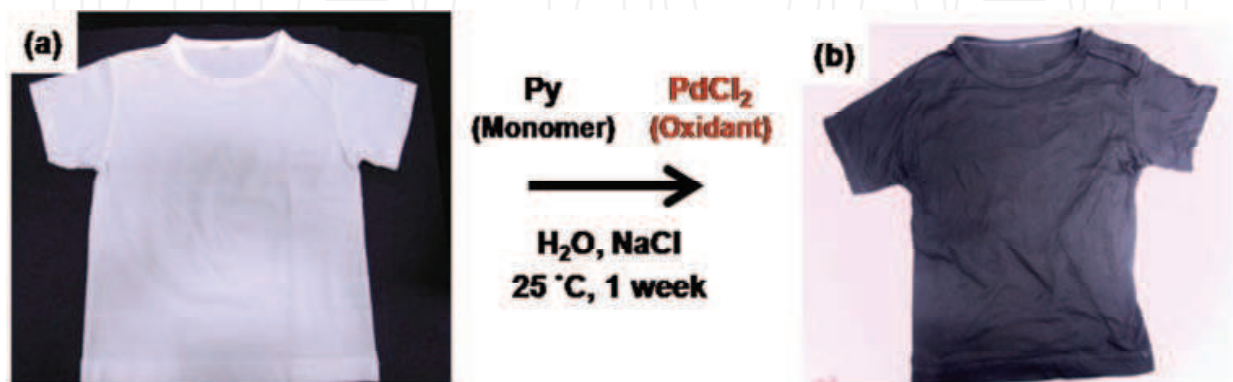Fig. 8. Optical micrographs of PPy-Pd nanocomposite-coated diacetate fibers with various PPy-Pd nanocomposite loadings after extraction of diacetate fiber with DMSO.

Fig. 9. Digital photographs of T-shirt (Cotton 100 %) before (a) and after (b) PPy-Pd nanocomposite coating.

3.2.1.2 PPy-Pt nanocomposite-coated polymeric fibers

The deposition of PPy-metal nanocomposite other than PPy-Pd nanocomposite on the polymeric fibers (diacetate, cotton, polyamide, silk, viscose and wool) has also been investigated. After addition of the $H_2PtCl_6 \cdot 6H_2O$ oxidant to the aqueous media containing fibers with dissolved pyrrole monomer, the polymerization system turned black within 10 min, which indicates the production of the PPy-Pt component. The morphology of the synthesized fibers was assessed by optical microscopy, which indicated no signs of appreciable destruction of morphologies in all fiber systems. The color of the fibers changed from white to black, which suggests a deposition of black colored PPy-Pt composite on the fibers. SEM studies revealed that micrometer-sized fibers with smooth surface were obtained after chemical oxidative polymerization in all fiber systems, which is different result comparing with those obtained for PPy-Pd nanocomposite coating system. 'Tubular' morphologies, with diameters corresponding to those of the original coated fibers, were observed using optical microscope after the extraction of core component from the composite fibers. This result confirms that the composite fibers do possess a core-shell morphology. The structure of PPy-Pt nanocomposite shell (pyrrole 100 wt%) was investigated using TEM in detail (Figure 10). The TEM image revealed the heterogeneous character of the shell is composed of a more transparent host PPy with incorporated Pt nanoparticles that have a higher absorbance for TEM electrons. The Pt nanoparticles have near-monodispersed size distributions and the number average diameters of the Pt nanoparticles were measured to be approximately 1 nm in all fiber systems. Other conducting polymer-metal nanocomposites such as PPy-silver, PANI-silver and PEDOT-Pd can also be deposited onto the fibers with maintaining fibrous morphology.
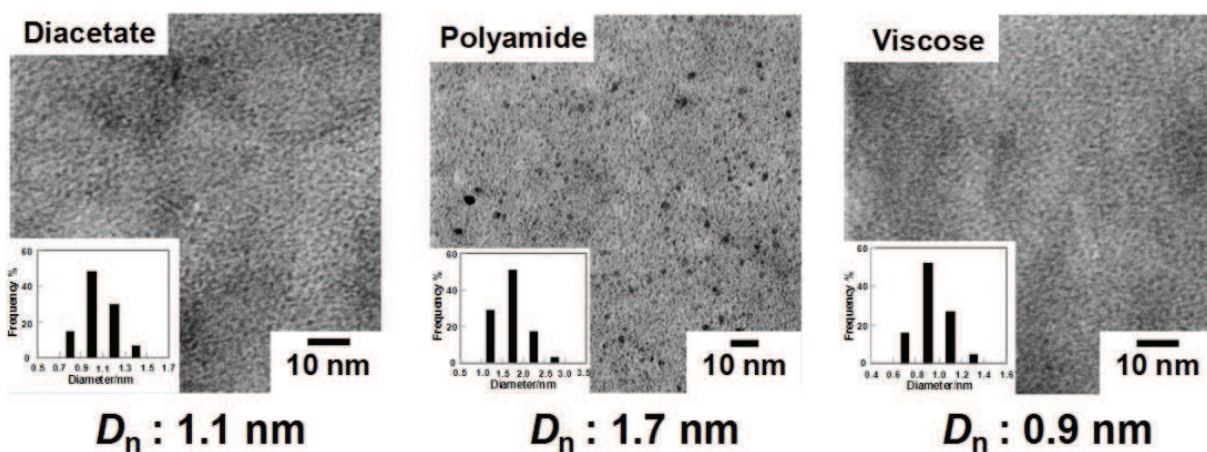

Fig. 10. TEM images of PPy-Pt nanocomposite-coated fibers after extraction of fibers. DMSO (for diacetate and viscose) and formic acid (for polyamide) were used for extraction of polymeric fibers.

3.2.2 Conducting polymer-metal nanocomposite coating on inorganic fibers

The deposition of PPy-Pd nanocomposite on the inorganic fibers has also been investigated. Here we used inorganic fibers made of silica and quarts. After chemical oxidative polymerization, the color of the fibers changed from white to black, which suggests a deposition of black colored PPy-Pd nanocomposite on the inorganic fibers. PPy-Pd

nanocomposite component precipitated in the aqueous media and on the fiber surface should accumulate on the fiber surface in order to minimize interfacial free energy (Lovell et al., 1997; Okubo et al., 1999). Interaction between silanol group on the fiber surface and cationic PPy should also play an important role for the PPy-Pd nanocomposite to deposit on the fiber surface (Maeda et al., 1994). SEM studies revealed that both quartz and silica fibers had submicrometer-sized dots (290 ~ 310 nm) on their surfaces and also the distinctive, micrometer-sized globular morphology of the PPy-Pd nanocomposite by-products with sizes between a few and 60 μm were formed as separate sub-phases (see Figure 11). The by-products seem to be the excessively precipitated PPy-Pd nanocomposites from the aqueous medium, which were entrapped between the fibers.

Nanocomposite coating can be easily scaled up: a microfiber thimble (2.5 cm in diameter and 9.0 cm in length) which consists of silica fibers was coated in its form. Digital camera images of the microfiber thimble before and after PPy-Pd nanocomposite coating by chemical oxidative polymerization in aqueous media at room temperature suggest that the color of the microfiber thimble changed from white to black, which indicates the nanocomposite coating. Using the microfiber thimbles, Pd-based catalytic reaction can be conducted in a continuous mode.
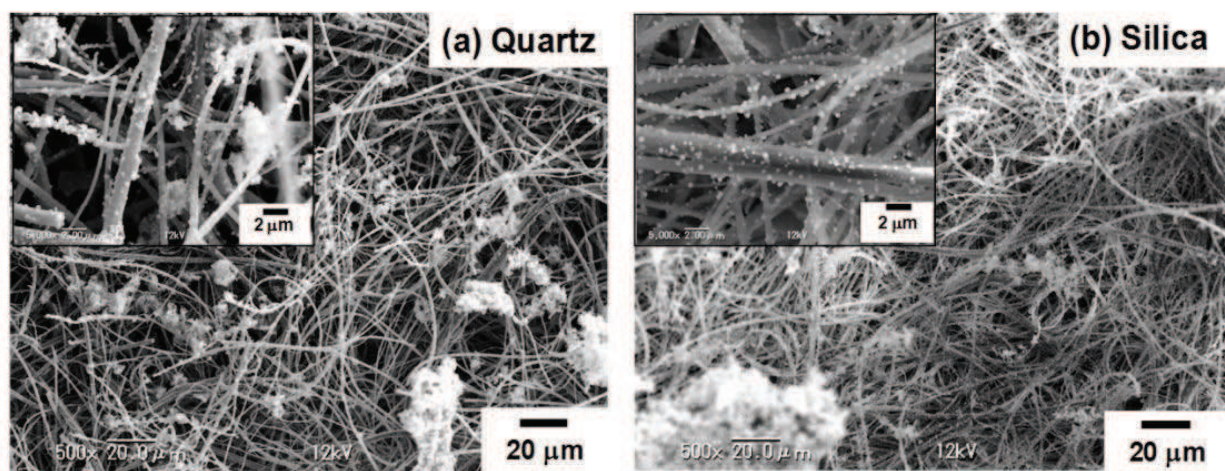

Fig. 11. SEM images of (a) quartz and (b) silica fibers after PPy-Pd nanocomposite coating (Py, 100 wt % based on fiber).

3.3 Suzuki coupling reactions using the conducting polymer-metal nanocomposite coated fibers as a catalyst

The Suzuki coupling reaction is an important and versatile method for the generation of unsymmetrical biaryls from aryl halides and arylboronic acids in a single step using Pd species as a catalyst (Miyaura et al., 1995; Hassan et al., 2002). The development of immobilized Pd catalysts and the use of aqueous media have been of great interest in recent organic chemistry (Lamblin et al., 2010). The simple recovery of catalysts by filtration and their reuses resulted in enhancing the economical evaluation of the reaction. At the same time, there is a prospect that the environmental pollution caused by residual metals in the waste fluid will be decreased. Pd nanoparticles are known to be effective catalysts for chemical transformations due to the high surface-to-volume ratio (Astruc et al., 2005; Moreno-Mañas et al., 2003). The common method to prepare Pd nanoparticles involves the

reduction of Pd(II) salt in the presence of stabilizers because they tend to precipitate or aggregate and lose their high catalytic activities. Hydrophilic polymers (Sawoo et al., 2009; Wei et al., 2008)- and hydrophobic polymers (Lyubimov et al., 2009)-stabilized Pd nanoparticles have high catalytic activity toward Suzuki coupling reaction in water.
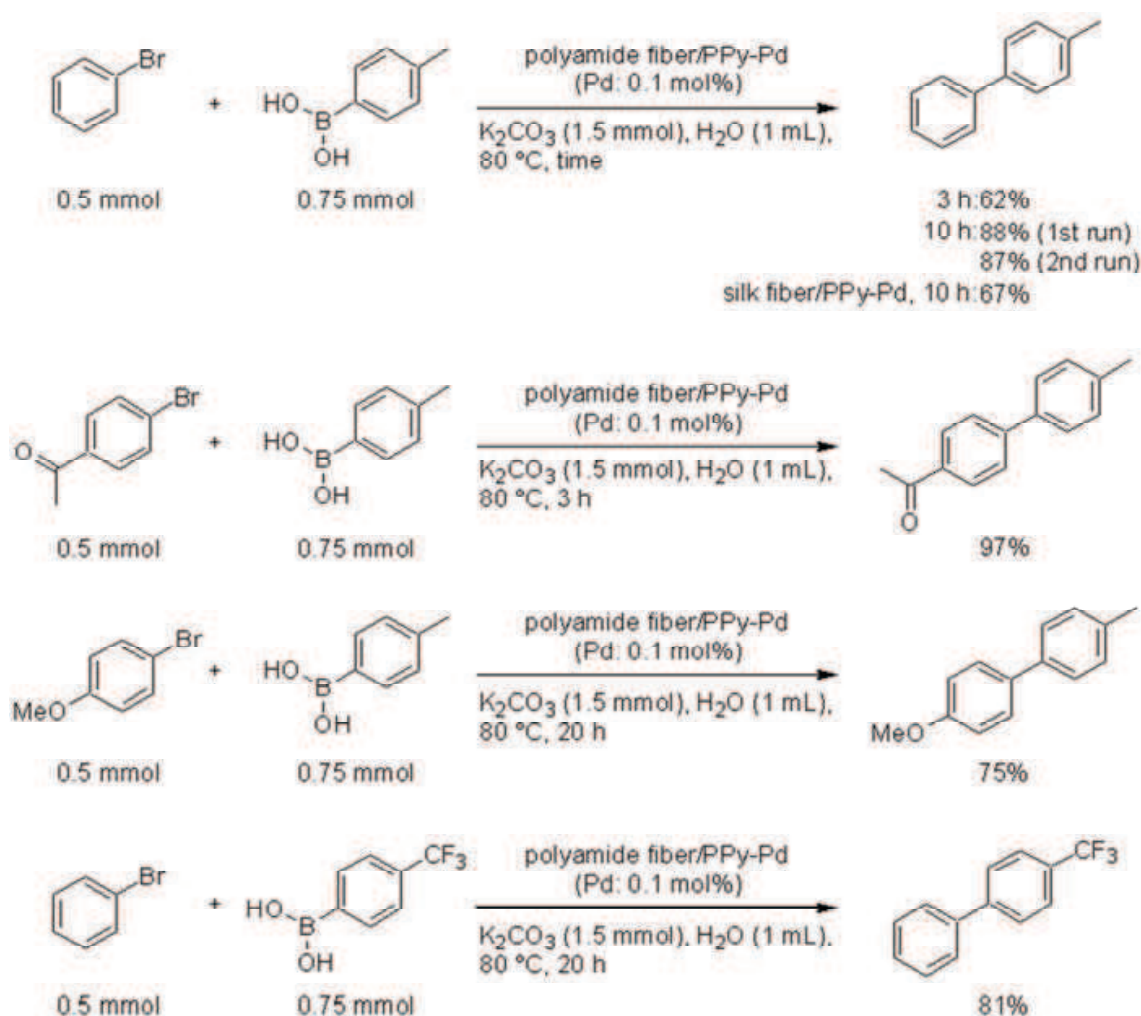
Scheme 3. Representative Suzuki-cross coupling reactions performed using the PPy-Pd nanocomposite-coated fibers as a catalyst.

However, a significant decrease in catalytic activity is observed for recycling because of a significant leaching of Pd into the reaction solutions and a decrease of Pd surface area caused by Ostwald ripening during the reaction. There have been several reports showing conducting polymers can be used as a support for Pd catalyst (Choudary et al., 2006; Houdayer et al., 2005). Kantam *et al.* reported that PANI-supported Pd nanoparticles have high catalytic activity for Suzuki coupling reactions in water and were reused without loss of activity (Kantam et al., 2007). PANI nanofiber-supported Pd nanoparticles with low metal loading (0.05 mol%) are active catalysts for the Suzuki coupling reaction of aryl chlorides with arylboronic acids in water (Gallon et al., 2007). Recently, we have found PPy-Pd nanocomposite-coated polystyrene particles have high catalytic activity for Suzuki coupling reaction in water (Fujii et al., 2010). Encouraged by this result, we examined the Suzuki coupling reaction using the PPy-Pd nanocomposite-coated fibers in aqueous media.

The reaction of bromobenzene with *p*-methylphenylboronic acid was carried out in 1.5 mol L^{-1} aqueous potassium carbonate solution in the presence of PPy-Pd nanocomposite-coated polyamide fiber (0.1 mol% of Pd) at 80 °C for 3 h to give 4-methylbiphenyl in 62 % yield. When the reaction time was extended to 10 h, the coupling product was obtained in 88% yield (Scheme 3). This result indicated that the PPy-Pd nanocomposite-coated polyamide fiber showed lower catalytic activity than the PPy-Pd nanocomposite-coated PS particles, probably due to smaller surface-to-volume ratio. After the reaction, the catalyst was recovered and reused under the same reaction conditions without significant loss of activity. 4-Bromoacetophenone (electron-deficient aryl bromide) also underwent the Suzuki coupling reaction with *p*-methylphenylboronic acid at 80 °C for 3 h to afford the corresponding product in 97% yield. Both *p*-bromoanisole (electron-rich aryl bromide) and *p*-(trifluoromethyl)phenylboronic acid (electron-deficient arylboronic acid) were reactive, affording the desired coupling products in 75% and 81% yields, respectively. These results indicate that the PPy-Pd nanocomposite-coated polyamide fibers are an effective catalyst for Suzuki reactions performed in aqueous media.

4. Conclusions

In summary, polymeric and inorganic fibers were successfully coated with an ultrathin layer of PPy-metal nanocomposite by aqueous chemical oxidative polymerization using metal salts as an oxidant in one step. The resulting composite fibers were extensively characterized using optical microscopy, SEM, TEM, XPS, XRD, FT-IR, elemental analysis, contact angle and electrical conductivity measurements. Extensive studies were conducted for the PPy-Pd nanocomposite-coated polymeric fibers. Good control over the PPy-Pd nanocomposite loading was demonstrated by simply varying the weight ratio of the fiber and pyrrole monomer. Optical microscopy study confirmed that the morphology of nanocomposite-coated fibers was not destroyed after PPy-Pd nanocomposite coating. SEM and TEM studies indicated the presence of PPy-Pd nanocomposite shells and revealed two Pd nanoparticle size distributions: 6.0-nm Pd nanoparticles forming 50-250 nm-sized Pd aggregates on the shell and 1.4-nm Pd nanoparticles dispersed in the shell. XPS studies provided an evidence for the presence of elemental Pd within/on the shell, in agreement with the TEM and contact angle measurement results. Solvent extraction of the fiber component led to the formation of PPy-Pd nanocomposite tubes, which also supported the core-shell morphology. Production of conducting polymer-metal nanocomposite-coated fibers in a large scale can be easily attained. The synthesized composite fibers were then tested for their catalytic activity in C-C bond formation. Suzuki coupling reactions performed in aqueous media demonstrated that PPy-Pd nanocomposite-coated fibers act as an efficient catalyst in organic chemistry. The advantages of a nanocomposite-coated fiber-based catalytic system are high activity, air and temperature stability and ease of separation. The fiber nanoengineering developed in this study provides a pathway to various practical hybrid materials with desired functions thanks to the rich varieties of natural/synthetic fibers, metals and conducting polymers.

5. Acknowledgments

6. References

Abidian, MR.; Kim, D.-H. & Martin, DC. (2006). Conducting-Polymer Nanotubes for Controlled Drug Release. *Advanced Materials,* Vol. 18, pp. 405-409

Andrieux, CP.; Dumasbouchiat, JM. & Saveant, JM. (1982). Catalysis of Electrochemical Reactions at Redox Polymer Electrodes: Kinetic Model for Stationary Voltammetric Techniques. *Journal of Electroanalytical Chemistry and Interfacial Electrochemistry,* Vol. 131, pp. 1-35

Appel, G.; Yfantis, A.; Göpel, W. & Schmeiβer, D. (1996). Highly Conductive Polypyrrole Films on Non-Conductive Substrates. *Synthetic Metals,* Vol. 83, pp. 197-200

Armes, SP.; Gottesfeld, S.; Beery, JG.; Garzon, F. & Agnew, SF. (1991). Conducting Polymer-Colloidal Silica Composites. *Polymer,* Vol. 32, pp. 2325-2330

Armes, SP. (1998). Chapter 17 in *Handbook of Conducting Polymers*, Marcel Dekker Inc, Ed. Elsenbaumer, RL.; Reynolds, JR.; Skotheim, TA. & Armes, SP. Colloidal Dispersions of Conducting Polymers, pp. 423-435

Astruc, D.; Lu, F. & Aranzaes, JR. (2005). Nanoparticles as Recyclable Catalysts: The Frontier between Homogeneous and Heterogeneous Catalysis. *Angewandte Chemie International Edition,* Vol. 44, pp. 7852-7872

Bjorklund, RB. & Liedberg, B. (1986). Electrically Conducting Composites of Colloidal Polypyrrole and Methylcellulose. *Journal of the Chemical Society, Chemical Communications*, pp. 1293-1295

Bull, RA.; Fan, F.-R. & Bard, AJ. (1983). Polymer Films on Electrodes. *Journal of the Electrochemical Society,* Vol. 130, pp. 1636-1638

Burroughes, JH.; Jones, CA. & Friend, RH. (1988). New Semiconductor Device Physics in Polymer Diodes and Transistors. *Nature,* Vol. 335, pp. 137–141

Chehimi, MM.; Azioune, A.; Bousalem, S.; Slimane, AB. & Yassar, A. (2004). Chapter 10 in *Colloidal Polymers: Synthesis and Characterization* (Surfactant Science Vol. 115) Marcel Dekker Inc, Edn. Elaissari, A.; Synthesis, Characterization, and Biomedical Applications of Conducting Polymer Particles, pp. 245-284

Chen, A.; Kamata, K.; Nakagawa, M.; Iyoda, T.; Wang, H. & Li, X. (2005). Formation Process of Silver−Polypyrrole Coaxial Nanocables Synthesized by Redox Reaction between $AgNO_3$ and Pyrrole in the Presence of Poly(vinyl pyrrolidone). *The Journal of Physical Chemistry B,* Vol. 109, pp. 18283-18288

Chen, A.; Wang, H. & Li, X. (2005). One-Step Process to Fabricate Ag–Polypyrrole Coaxial Nanocables. *Chemical Communications*, pp. 1863-1864

Choudary, BM.; Roy, M.; Roy, S.; Kantam, ML.; Sreedhar, B. & Kumar, KV. (2006). Preparation, Characterization and Catalytic Properties of Polyaniline-Supported Metal Complexes. *Advanced Synthesis & Catalysis,* Vol. 348, pp. 1734-1742

Collins, GE. & Buckley, LJ. (1996). Conductive Polymer-Coated Fabrics for Chemical Sensing. *Synthetic Metals,* Vol. 78, pp. 93-101

Conway, BE. (1991). Transition from "Supercapacitor" to "Battery" Behavior in Electrochemical Energy Storage. *Journal of the Electrochemical Society,* Vol. 138, pp. 1539-1548

Dong, H.; Nyame, V.; MacDiarmid, AG. & Jones, WE. Jr. (2004). Polyaniline/Poly(methyl methacrylate) Coaxial Fibers: The Fabrication and Effects of the Solution Properties on the Morphology of Electrospun Core Fibers. *Journal of Polymer Science Part B: Polymer Physics,* Vol. 42, pp. 3934–3942

Dong, H.; Prasad, S.; Nyame, V. & Jones, WE. Jr. (2004). Sub-Micrometer Conducting Polyaniline Tubes Prepared from Polymer Fiber Templates. *Chemistry of Materials,* Vol. 16, pp. 371-373

Drelinkiewicz, A.; Hasik, M. & Kloc, M. (2000). Pd/Polyaniline as the Catalysts for 2-Ethylanthraquinone Hydrogenation. The Effect of Palladium Dispersion. *Catalysis Letters*, Vol. 64, pp. 41-47

Freund, MS. & Lewis, NS. (1995). A Chemically Diverse Conducting Polymer-Based "Electronic Nose". *Proceedings of the National Academy of Sciences of the United States of America,* Vol. 92, pp. 2652-2656

Fujii, S.; Aichi, A.; Akamatsu, K.; Nawafune, H. & Nakamura, Y. (2007). One-Step Synthesis of Polypyrrole-Coated Silver Nanocomposite Particles and Their Application as a Coloured Particulate Emulsifier. *Journal of Materials Chemistry,* Vol. 17, pp. 3777-3779

Fujii, S.; Mouri, M.; Aichi, A.; Akamatsu, K.; Nawafune, H. & Nakamura, Y. (2008). Synthesis of Polypyrrole-Gold Nanocomposite-Coated Polystyrene Latex Particles by Simultaneous Organic-Inorganic Deposition Method. *Journal of the Adhesion Society of Japan,* Vol. 44, pp. 12-18

Fujii, S.; Matsuzawa, S.; Nakamura, Y.; Ohtaka, A.; Teratani, T.; Akamatsu, K.; Tsuruoka, T. & Nawafune, H. (2010). Synthesis and Characterization of Polypyrrole−Palladium Nanocomposite-Coated Latex Particles and Their Use as a Catalyst for Suzuki Coupling Reaction in Aqueous Media. *Langmuir,* Vol. 26, pp. 6230-6239

Fujii, S.; Nishimura, Y.; Aichi, A.; Matsuzawa, S.; Nakamura, Y.; Akamatsu, K. & Nawafune, H. (2010). Facile One-Step Route to Polyaniline–Silver Nanocomposite Particles and Their Application as a Colored Particulate Emulsifier. *Synthetic Metals*, Vol. 160, pp. 1433-1437

Gallon, BJ.; Kojima, RW.; Kaner, RB. & Diaconescu, PL. (2007). Palladium Nanoparticles Supported on Polyaniline Nanofibers as a Semi-Heterogeneous Catalyst in Water. *Angewandte Chemie International Edition,* Vol. 46, pp. 7251-7254

Gangopadhyay, R. & De, A. (2000). Conducting Polymer Nanocomposites: A Brief Overview. *Chemistry of Materials,* Vol. 12, pp. 608-622

Gardner, JW. & Bartlett, PN. (1993). Design of Conducting Polymer Gas Sensors: Modelling and Experiment. *Synthetic Metals,* Vol. 57, pp. 3665-3670

Geniès, EM. (1991). *New Journal of Chemistry*, Vol. 15, pp. 373-377

Gregory, RV.; Kimbrell, WC. & Kuhn, HH. (1989). Conductive Textiles. *Synthetic Metals,* Vol. 28, pp. 823-835

Grimaldo, EB.; Hachey, S.; Cameron, CG. & Freund, MS. (2007). Metastable Reaction Mixtures for the in situ Polymerization of Conducting Polymers. *Macromolecules*, Vol. 40, pp. 7166-7170

Guimard, NK.; Gomez, N. & Schmidt, CE. (2007). Conducting Polymers in Biomedical Engineering. *Progress in Polymer Science*, Vol. 32, pp. 876-921

Gustafsson, G.; Cao, Y.; Treacy, GM.; Klavetter, F.; Colaneri, N. & Heeger, A. (1992). Flexible Light-Emitting Diodes Made from Soluble Conducting Polymers. *Nature,* Vol. 357, pp. 477-479

Hable, CT. & Wrighton, MS. (1993). Electrocatalytic Oxidation of Methanol and Ethanol: a Comparison of Platinum-Tin and Platinum-Ruthenium Catalyst Particles in a Conducting Polyaniline Matrix. *Langmuir,* Vol. 9, pp. 3284-3290

Han, C.-C.; Lee. J.-T.; Yang, R.-W.; Chang, H. & Han, C.-H. (1999). A New and Easy Method for Making Well-Organized Micrometer-Sized Carbon Tubes and Their Regularly Assembled Structures. *Chemistry of Materials,* Vol. 11, pp.1806-1813

Han, C.-C.; Lee, J.-T.; Yang, R.-W. & Han C.-H. (2001). Formation Mechanism of Micrometer-Sized Carbon Tubes. *Chemistry of Materials,* Vol. 13, pp. 2656–2665

Hassan, J.; Sevignon, M.; Gozzi, C.; Schulz, E. & Lemaire, M. (2002). Aryl-Aryl Bond Formation One Century after the Discovery of the Ullmann Reaction. *Chemical Reviews*, Vol. 102, pp. 1359-1469

Heisey, CL.; Wightman, JP.; Pittman, EH. & Kuhn, HH. (1993). Surface and Adhesion Properties of Polypyrrole-Coated Textiles. *Textile Research Journal*, Vol. 63, pp.247-256

Heller, A. (1992). Electrical Connection of Enzyme Redox Centers to Electrodes. *The Journal of Physical Chemistry,* Vol. 96, pp. 3579-3587

Henry, MC.; Hsueh, C.-C.; Timko, BP. & Freund, MS. (2001). Reaction of Pyrrole and Chlorauric Acid a New Route to Composite Colloids. *Journal of the Electrochemical Society,* Vol. 148, pp. D155-D162

Houdayer, A.; Schneider, R.; Billaud, D. & Ghanbaja, J. (2005). Heck and Suzuki-Miyaura Couplings Catalyzed by Nanosized Palladium in Polyaniline. *Applied Organometallic Chemistry,* Vol. 19, pp. 1239-1248

Huang, J.; Ichinose, I. & Kunitake, T. (2005). Nanocoating of Natural Cellulose Fibers with Conjugated Polymer: Hierarchical Polypyrrole Composite Materials. *Chemical Communications*, pp. 1717-1719

Josowicz, M. & Janata, J. (1986). Suspended Gate Field Effect Transistors Modified with Polypyrrole as Alcohol Sensor. *Analytical. Chemistry,* Vol. 58, pp. 514-517

Kantam, ML.; Roy, M.; Roy, S.; Sreedhar, B.; Madhavendra, SS.; Choudary, BM. & De, RL. (2007). Polyaniline Supported Palladium Catalyzed Suzuki-Miyaura Cross-Coupling of Bromo- and Chloroarenes in Water. *Tetrahedron,* Vol. 63, pp. 8002-8009

Kaynak, A.; Wang, L.; Hurren, C. & Wang, X. (2002). Characterization of Conductive Polypyrrole Coated Wool Yarns. *Fibers and Polymers,* Vol. 3, pp. 24-30

Kim, SM.; Kim HK.; Byun, SW.; Jeong, SH.; Hong YK.; Joo, JS.; Song, KT.; Kim, JK.; Lee, CJ. & Lee, JY. (2002). PET Fabric/Polypyrrole Composite with High Electrical Conductivity for EMI Shielding. *Synthetic Metals,* Vol. 126, pp. 233-239

Kincal, D.; Kumar, A.; Child, AD. & Reynolds, JR. (1998). Conductivity Switching in Polypyrrole-Coated Textile Fabrics as Gas Sensors. *Synthetic Metals,* Vol. 92, pp. 53-56

Kitani, A.; Akashi, T.; Sugimoto, K. & Ito, S. (2001). Electrocatalytic Oxidation of Methanol on Platinum Modified Polyaniline Electrodes. *Synthetic Metals,* Vol. 121, pp. 1301-1302

Kuhn, HH.; Child, AD. & Kimbrell, WC. (1995). Toward Real Applications of Conductive Polymers. *Synthetic Metals,* Vol. 71, pp. 2139-2142

Kuwabata, S. & Martin, CR. (1994). Mechanism of the Amperometric Response of a Proposed Glucose Sensor Based on a Polypyrrole-Tubule-Impregnated Membrane. *Analytical Chemistry,* Vol. 66, pp. 2757-2762

Lamblin, M.; Nassar-Hardy, L.; Hierso, J.-C.; Fouquet, E. & Felpin, F.-X. (2010). Recyclable Heterogeneous Palladium Catalysts in Pure Water: Sustainable Developments in Suzuki, Heck, Sonogashira and Tsuji-Trost Reactions. *Advanced Synthesis & Catalysis,* Vol. 352, pp. 33-79

Lascelles, SF. & Armes, SP. (1997). Synthesis and Characterization of Micrometre-Sized, Polypyrrole-Coated Polystyrene Latexes. *Journal of Materials Chemistry,* Vol. 7, pp. 1339-1347

Li, F. & Albery, WJ. (1991). Electrochemical Polymerization of Poly(thiophene-3-ethyl acetate) — a New Candidate for a Rechargeable Battery Cathode. *Journal of Electroanalytical Chemistry and Interfacial Electrochemistry,* Vol. 302, pp. 279-284

Lovell, PA. & El-Aasser. MS. (1997). *Emulsion Polymerization and Emulsion Polymers.* John Wiley and Sons, Chichester, UK

Lyubimov, SE.; Vasil'ev, AA.; Korlyukov, AA.; Ilyin, MM.; Pisarev, SA.; Matveev, VV.; Chalykh, AE.; Zlotin, SG. & Davankov, VA. (2009). Palladium-Containing Hypercrosslinked Polystyrene as an Easy to Prepare Catalyst for Suzuki Reaction in Water and Organic Solvents. *Reactive & Functional Polymers,* Vol. 69, pp. 755-75

Maeda, S. & Armes, SP. (1994). Preparation and Characterisation of Novel Polypyrrole–Silica Colloidal Nanocomposites. *Journal of Materials Chemistry,* Vol. 4, pp. 935-94

Miller, LL. (1988). Electrochemically Controlled Release of Drug Ions from Conducting Polymers. *Molecular Crystals and Liquid Crystals,* Vol. 160, pp. 297-301

Miyaura, N. & Suzuki, A. (1995). Palladium-Catalyzed Cross-Coupling Reactions of Organoboron Compounds. *Chemical Reviews*, Vol. 95, pp. 2457-2483

Moreno-Mañas, M. & Pleixats, R. (2003). Formation of Carbon-Carbon Bonds under Catalysis by Transition-Metal Nanoparticles. *Accounts of Chemical Research,* Vol. 36, pp. 638-643

Niwa, O. & Tamamura, T. (1984). Electrochemical Polymerization of Pyrrole on Polymer-Coated Electrodes. *Journal of the Chemical Society, Chemical Communications,* pp. 817-818

Niwa, O.; Kakuchi, M. & Tamamura, T. (1987). Polypyrrole-Based Conducting Polymer Alloy Films: Physical Properties and Film Morphology. *Macromolecules*, Vol. 20, pp. 749-753

Oh, KW.; Hong, KH. & Kim, SH. (1999). Electrically Conductive Textiles by *in situ* Polymerization of Aniline. *Journal of Applied Polymer Science,* Vol. 74, pp. 2094-210

Okubo, M.; Izumi, J. & Takekoh, R. (1999). Production of Micron-Sized Monodispersed Core/Shell Composite Polymer Particles by Seeded Dispersion Polymerization. *Colloid and Polymer Science,* Vol. 277, pp. 875-880

Okubo, M.; Fujii, S. & Minami, H. (2001). Production of Electrically Conductive, Core/Shell Polystyrene/Polyaniline Composite Particles by Chemical Oxidative Seeded Dispersion Polymerization. *Colloid and Polymer Science,* Vol. 279, pp. 139-145

Paoli, M.-AD.; Waltman, RJ.; Diaz, AF. & Bargon, J. (1984). Conductive Composite From Poly(vinyl chloride) and Polypyrrole. *Journal of the Chemical Society, Chemical Communications,* pp. 1015-1016

Pillalamarri, SK.; Blum, FD.; Tokuhiro, AT. & Bertino, MF. (2005). One-Pot Synthesis of Polyaniline−Metal Nanocomposites. *Chemistry of Materials,* Vol. 17, pp. 5941-5944

Radford, PT. & Creager, SE. (2001). Dual-Stream Flow Injection Method for Amplified Electrochemical Detection of Ferrocene Ferivatives. *Analytica Chimica Acta,* Vol. 449, pp. 199-209

Sailor, MJ.; Ginsburg, EJ.; Gorman, CB., Kumar, A.; Grubbs, RH. & Lewis, NS. (1990). Thin Films of n-Si/Poly-$(CH_3)_3$Si-Cyclooctatetraene: Conducting-Polymer Solar Cells and Layered Structures. *Science,* Vol. 249, pp. 1146-1149

Sawoo, S.; Srimani, D.; Dutta, P.; Lahiri, R. & Sarkar, A. (2009). Size Controlled Synthesis of Pd Nanoparticles in Water and Their Catalytic Application in C-C Coupling Reactions. *Tetrahedron,* Vol. 65, pp. 4367-4374

Selvan, ST.; Spatz, JP.; Klok, H.-A. & Möller, M. (1998). Gold–Polypyrrole Core–Shell Particles in Diblock Copolymer Micelles. *Advanced Materials,* Vol. 10, pp. 132–134

Tian, ZQ.; Lian, YZ.; Wang, JQ.; Wang, SJ. & Li, WH. (1991). Electrochemical and XPS Studies on the Generation of Silver Clusters in Polyaniline Films. *Journal of Electroanalytical Chemistry and Interfacial Electrochemistry,* Vol. 308, pp. 357-363

Vasilyeva, SV.; Vorotyntsev, MA.; Bezverkhyy, I.; Lesniewska, E.; Heintz, O. & Chassagnon, R. (2008). Synthesis and Characterization of Palladium Nanoparticle/Polypyrrole Composites. *The Journal of Physical Chemistry C,* Vol. 112, pp. 19878-19885

Wang, G.; Swensen, J.; Moses, D. & Heeger, AJ. (2003). Increased Mobility from Regioregular Poly(3-hexylthiophene) Field-Effect Transistors. *Journal of Applied Physics,* Vol. 93, pp. 6137-6141

Wei, G.; Zhang, W.; Wen, F.; Wang, Y. & Zhang, M. (2008). Suzuki Reaction within the Core-Corona Nanoreactor of Poly(*N*-isopropylacrylamide)-Grafted Pd Nanoparticle in Water. *The Journal of Physical Chemistry C,* Vol. 112, pp. 10827-10832

Wen, F.; Zhang, W.; Wei, G.; Wang, Y.; Zhang, J.; Zhang, M. & Shi, L. (2008). Synthesis of Noble Metal Nanoparticles Embedded in the Shell Layer of Core−Shell Poly(styrene-*co*-4-vinylpyridine) Micospheres and Their Application in Catalysis. *Chemistry of Materials,* Vol. 20, pp. 2144–2150

Yosomiya, R.; Hirata, M.; Haga, Y.; An, H. & Seki, M. (1986). Electrical Properties of Polypyrrole-Polymer Composite Films. *Die Makromolekulare Chemie, Rapid Communications,* Vol. 7, pp. 697-701

Zhang, C.; Hoger, S.; Pakbaz, K.; Wudl, F. & Heeger, AJ. (1994). Improved Efficiency in Green Polymer Light-Emitting Diodes with Air-Stable Electrodes. *Journal of Electronic Materials,* Vol. 23, pp. 453-458

Zhang, M. & Zhang, W. (2008). Pd Nanoparticles Immobilized on pH-Responsive and Chelating Nanospheres as an Efficient and Recyclable Catalyst for Suzuki Reaction in Water. *The Journal of Physical Chemistry C,* Vol. 112, pp. 6245-6252
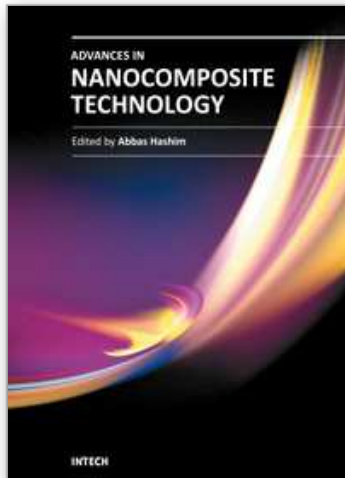
Advances in Nanocomposite Technology

Edited by Dr. Abbass Hashim

The book "Advances in Nanocomposite Technology" contains 16 chapters divided in three sections. Section one, "Electronic Applications", deals with the preparation and characterization of nanocomposite materials for electronic applications and studies. In section two, "Material Nanocomposites", the advanced research of polymer nanocomposite material and polymer-clay, ceramic, silicate glass-based nanocomposite and the functionality of graphene nanocomposites is presented. The "Human and Bioapplications" section is describing how nanostructures are synthesized and draw attention on wide variety of nanostructures available for biological research and treatment applications. We believe that this book offers broad examples of existing developments in nanocomposite technology research and an excellent introduction to nanoelectronics, nanomaterial applications and bionanocomposites.

How to reference

In order to correctly reference this scholarly work, feel free to copy and paste the following:

Syuji Fujii, Mizuho Kodama, Soichiro Matsuzawa, Hiroyuki Hamasaki, Atsushi Ohtaka and Yoshinobu Nakamura (2011). Conducting Polymer-Metal Nanocomposite Coating on Fibers, Advances in Nanocomposite Technology, Dr. Abbass Hashim (Ed.), ISBN: 978-953-307-347-7, InTech, Available from: http://www.intechopen.com/books/advances-in-nanocomposite-technology/conducting-polymer-metal-nanocomposite-coating-on-fibers

INTECH
open science | open minds